ORIGINAL ARTICLE

Association of HTRA1 Mutations and Familial Ischemic Cerebral Small-Vessel Disease

Kenju Hara, M.D., Ph.D., Atsushi Shiga, M.Med., Toshio Fukutake, M.D., Ph.D., Hiroaki Nozaki, M.D., Akinori Miyashita, Ph.D., Akio Yokoseki, M.D., Hirotoshi Kawata, M.D., Ph.D., Akihide Koyama, M.Med., Kunimasa Arima, M.D., Ph.D., Toshiaki Takahashi, M.D., Ph.D., Mari Ikeda, M.Med., Hiroshi Shiota, M.D., Ph.D., Masato Tamura, M.D., Ph.D., Yutaka Shimoe, M.D., Ph.D., Mikio Hirayama, M.D., Ph.D., Takayo Arisato, M.D., Ph.D., Sohei Yanagawa, M.D., Ph.D., Akira Tanaka, M.D., Ph.D., Imaharu Nakano, M.D., Ph.D., Shu-ichi Ikeda, M.D., Ph.D., Yutaka Yoshida, Ph.D., Tadashi Yamamoto, M.D., Ph.D., Takeshi Ikeuchi, M.D., Ph.D., Ryozo Kuwano, M.D., Ph.D., Masatoyo Nishizawa, M.D., Ph.D., Shoji Tsuji, M.D., Ph.D., and Osamu Onodera, M.D., Ph.D.

ABSTRACT

BACKGROUND

The genetic cause of cerebral autosomal recessive arteriopathy with subcortical infarcts and leukoencephalopathy (CARASIL), which is characterized by ischemic, nonhypertensive, cerebral small-vessel disease with associated alopecia and spondylosis, is unclear.

METHODS

In five families with CARASIL, we carried out linkage analysis, fine mapping of the region implicated in the disease, and sequence analysis of a candidate gene. We also conducted functional analysis of wild-type and mutant gene products and measured the signaling by members of the transforming growth factor β (TGF-β) family and gene and protein expression in the small arteries in the cerebrum of two patients with CARASIL.

RESULTS

We found linkage of the disease to the 2.4-Mb region on chromosome 10q, which contains the HtrA serine protease 1 (HTRA1) gene. HTRA1 is a serine protease that represses signaling by TGF-β family members. Sequence analysis revealed two nonsense mutations and two missense mutations in HTRA1. The missense mutations and one of the nonsense mutations resulted in protein products that had comparatively low levels of protease activity and did not repress signaling by the TGF-β family. The other nonsense mutation resulted in the loss of HTRA1 protein by nonsense-mediated decay of messenger RNA. Immunohistochemical analysis of the cerebral small arteries in affected persons showed increased expression of the extra domain–A region of fibronectin and versican in the thickened tunica intima and of TGF-β1 in the tunica media.

CONCLUSIONS

CARASIL is associated with mutations in the HTRA1 gene. Our findings indicate a link between repressed inhibition of signaling by the TGF-β family and ischemic cerebral small-vessel disease, alopecia, and spondylosis.

From Niigata University, Niigata (K.H., A.S., H.N., A.M., A.Y., A.K., T.T., M.I., Y.Y., T.Y., T.I., R.K., M.N., O.O.); Kameda Medical Center, Kamogawa City (T.F.); Jichi Medical University, Tochigi (H.K., A.T., I.N.); National Center of Neurology and Psychiatry, Tokyo (K.A.); Nihon University School of Medicine, Tokyo (H.S.); Nagaoka-Nishi Hospital, Nagaoka (M.T.); Kashima Rosai Hospital, Kashima (Y.S.); Kasugai Municipal Hospital, Kasugai (M.H.); Minamikyushu National Hospital, Kagoshima (T.A.); Iida Municipal Hospital, Iida (S.Y.); Shinshu University School of Medicine, Matsumoto (S.I.); and University of Tokyo, Tokyo (S.T.) — all in Japan. Address reprint requests to Dr. Onodera at the Brain Research Institute, Niigata 951-8585, Japan, or at onodera@bri.niigata-u.ac.jp.

Dr. Hara and Mr. Shiga contributed equally to this article.

N Engl J Med 2009;360:1729-39.

HYPERTENSION IS A WELL-KNOWN RISK factor for nonhereditary cerebral small-vessel disease.[1] Genetic causes have been identified for hereditary cerebral small-vessel diseases — cerebral autosomal dominant arteriopathy with subcortical infarcts and leukoencephalopathy,[2] autosomal dominant retinal vasculopathy with cerebral leukodystrophy,[3] brain small-vessel disease with hemorrhage,[4] and familial cerebral amyloid angiopathy.[5] Although arteriopathy in these cerebral small-vessel diseases is well documented, little is known about its genetic basis.

Cerebral autosomal recessive arteriopathy with subcortical infarcts and leukoencephalopathy (CARASIL) is characterized by nonhypertensive cerebral small-vessel arteriopathy with subcortical infarcts, alopecia, and spondylosis, with an onset in early adulthood.[6-8] On neuropathological examination, arteriosclerosis associated with intimal thickening and dense collagen fibers, loss of vascular smooth-muscle cells, and hyaline degeneration of the tunica media has been observed in cerebral small arteries.[7-9] These pathological findings resemble those seen in patients with nonhereditary ischemic cerebral small-vessel disease.[7-11] We conducted a study to determine whether mutations in *HTRA1*, a gene encoding HtrA serine protease 1, cause CARASIL.

METHODS

SUBJECTS AND GENETIC ANALYSIS

We enrolled a total of six probands from six consanguineous families of Japanese ancestral origin and some of their family members. The first five families were included in a linkage analysis, and one member of the fifth family and one of the sixth family underwent neuropathological examination. Ancestry was reported by the participant or family members.

We isolated genomic DNA from 11 subjects from five of the families with CARASIL: 5 probands, 3 unaffected siblings, and 3 parents. We performed a genomewide linkage analysis using 763 microsatellite markers (Applied Biosystems). Pairwise lod scores were calculated with the MLINK program of the LINKAGE software package (version 5.2) and the FASTLINK package (version 4.1).[12,13] We established five new microsatellite markers — *M1236*, *M1238*, *M1241*, *M1260*, and *M1264* — on the basis of simple-repeat information from the University of California, Santa Cruz, Human Genome Browser. Primer sequences of these markers are summarized in the Supplementary Appendix (available with the full text of this article at NEJM.org). We designed primer pairs for amplification of the nine coding exons of *HTRA1*.

We isolated genomic DNA from all participants, including healthy persons of Japanese ancestral origin, as determined by means of self-report. These control subjects were between 74 and 90 years of age and had no signs of dementia, as defined by the Mini–Mental State Examination. We obtained fibroblast specimens from four controls and from Subject II-2 in Family 1.

We obtained written informed consent from the affected persons and their family members and written informed consent from the controls. The institutional review board of Niigata University approved this study.

ASSAY OF HTRA1 PROTEASE ACTIVITY

To express HTRA1 in *Escherichia coli* as fusions with glutathione S-transferase, we subcloned wild-type or mutant *HTRA1* complementary DNA (cDNA), lacking codons 1 through 140, into the vector pGEX 6P-3 (GE Healthcare). The N-terminus of HTRA1 is toxic to *E. coli*. Amino acid substitution of the serine protease motif S328A, which abolishes the protease activity in HTRA1, was used as a negative control.[14] Glutathione *S*-transferase fusion proteins were overexpressed and purified. Protease activity, measured as fluorescein isothiocyanate–labeled substrate β-casein, was evaluated with the use of a QuantiCleave Fluorescent Protease Assay Kit (Pierce) and recombinant glutathione *S*-transferase–HTRA1. To eliminate the possibility that a deletion of the N-terminus in HTRA1 affects protease activity, we also performed the identical protease assay using the serum-free medium containing cells stably expressing full-length wild-type or mutant HTRA1 tagged with a green fluorescent protein at the C-terminus. Green fluorescent protein–tagged HTRA1 proteins were detected by means of anti–green fluorescent protein antibody (Medical and Biological Laboratories, Nagoya, Japan).

To assay the formation of a stable complex with α_1-antitrypsin, we transiently expressed α_1-antitrypsin and either wild-type or mutated *HTRA1* cDNA with a simian virus 5 peptide (V5) tag at the C-terminus in the human embryonic kidney cell line HEK293. These cells were grown in serum-free medium, and samples of the resul-

tant conditioned medium were then immunoblotted with anti–V5 antibody.[14]

EXPRESSION OF *HTRA1* AND *NOG*

Total RNA was isolated from specimens of whole blood or cultured skin fibroblasts, and cDNA was synthesized with the use of the High-Capacity cDNA Reverse Transcription kit (Applied Biosystems). We assayed the expression of *HTRA1* messenger RNA (mRNA) in whole-blood samples by using gene-specific primers for *HTRA1*. To assay *HTRA1* mRNA levels in cultured skin fibroblasts in relation to the expression of glyceraldehyde-3-phosphate dehydrogenase, we performed a real-time quantitative reverse-transcriptase polymerase-chain-reaction (RT-PCR) assay by using specific TaqMan probes and primer sets (Applied Biosystems). We assayed mRNA levels of the noggin gene (*NOG*) in cultured skin fibroblasts in relation to the levels of β-actin by using real-time quantitative RT-PCR and SYBR Green (Applied Biosystems) (for details, see the Methods section of the Supplementary Appendix).

ASSAY OF SIGNALING BY TGF-β FAMILY PROTEINS

We used a site-directed mutagenesis system (GeneTailor, Invitrogen) to synthesize cDNA encoding mutant HTRA1 and cDNA encoding a constitutively active TGF-β1 proprotein (pro–TGF-β1 containing the activating amino acid mutations C223S and C225S).[15] We then individually subcloned this cDNA into the vector pcDNA DEST-40 (Invitrogen). Constitutively active TGF-β1 was synthesized from pro–TGF-β1 containing the activating mutations C223S and C225S. We isolated cDNA from the SMAD family member 2 gene (*SMAD2*), obtained from a library of human whole-brain cDNA (Clontech), and subcloned it into the pcDNA DEST-40 vector. Luciferase assays were performed as previously described.[16,17] Mouse C2C12 myoblasts (mesenchymal precursor cells, obtained from the American Type Culture Collection) were cotransfected with HTRA1-expression vectors, the pRL-TK renilla luciferase expression plasmid, and the following constructs: the (Smad binding element)$_4$–firefly luciferase vector (TGF-β–responsive reporter vector) and vectors containing *SMAD2*, the SMAD family member 4 gene (*SMAD4*), and *TGFB1* (encoding pro–TGF-β1 with the two point mutations C223S and C225S)[15]; the pGL3-Id985WT–firefly luciferase vector (bone morphogenetic protein [BMP]–responsive reporter vector)[17] and vectors containing the SMAD family member 1 gene (*SMAD1*), *SMAD4*, and *BMP-4* (encoding pro–BMP-4); and the pGL3-Id985WT–firefly luciferase vector[17] and vectors containing *SMAD1*, *SMAD4*,

Table 1. Clinical Characteristics of the Six Probands with CARASIL.*

Characteristic	Proband and Family No.					
	II-2, Family 1	II-3, Family 2	II-1, Family 6	II-7, Family 3	II-3, Family 4	II-3, Family 5
Consanguinity of family	Yes	Yes	Yes	Yes	Yes	Yes
Mutation (nucleotide and amino acid)	1108C→T R370X	904C→T R302X	904C→T R302X	889G→A V297M	889G→A V297M	754G→A A252T
Sex	Female	Male	Female	Female	Male	Female
Age at time of study (yr)	44	28	46	50	33	48
Age at onset (yr)	18	16	14	16	14	Teens
Initial symptom	Alopecia	Alopecia	Alopecia	Alopecia	Alopecia	Lumbago
Leukoaraiosis on brain MRI	Yes	Yes	Yes	Yes	Yes	Yes
Alopecia, age at onset (yr)	18	16	14	16	14	—
Spondylosis, age at onset (yr)	21	21	29	39	33	Teens
Dementia, age at onset (yr)	35	37	29	50	33	—
Acute stroke, age at onset (yr)	—	31	—	—	—	38
Gait disturbance, age at onset (yr)	35	26	32	31	29	38
Pseudobulbar palsy, age at onset (yr)	35	26	32	50	33	38
Pyramidal sign, age at onset (yr)	35	27	32	50	29	48
Hypertension	No	No	No	No	No	No

* None of the patients had hypertension, any cancer, abnormalities in the retinal artery, or macular degeneration. CARASIL denotes cerebral autosomal recessive arteriopathy with subcortical infarcts and leukoencephalopathy, and MRI magnetic resonance imaging.

and *BMP-2* (encoding pro–BMP-2).[18] Cell extracts were assayed for luciferase activity with the use of the Dual-Luciferase Reporter Assay System (Promega). The luciferase activity was corrected for transfection efficiency by dividing it by the pRL-TK renilla luciferase activity. Every sample was transfected in triplicate, and every experiment was repeated three times.

PHOSPHORYLATION OF SMAD PROTEINS

HEK293 cells were cotransfected with vectors containing *HTRA1* and the following constructs: vectors containing *SMAD2*, *SMAD4*, and *TGFB1* (encoding pro–TGF-β1 with two point mutations [C223S and C225S]); vectors containing *SMAD1*, *SMAD4*, and *BMP-4*; and vectors containing *SMAD1*, *SMAD4*, and *BMP-2*.[15,18] The cells were lysed in radioimmunoprecipitation assay buffer containing phosphatase inhibitor. We performed Western blotting to detect SMAD1, phosphorylated SMAD1, SMAD2, and phosphorylated SMAD2, using the corresponding anti-SMAD antibodies (Cell Signaling): anti-SMAD1, anti–phospho-SMAD1/5/8, anti-SMAD 2/3, and anti–phospho-SMAD2 antibodies.

IMMUNOHISTOCHEMICAL STUDIES AND IN SITU HYBRIDIZATION

We carried out immunoperoxidase staining on formalin-fixed, paraffin-embedded brain specimens obtained from two patients with CARASIL and from four controls (a 40-year-old woman with amyotrophic lateral sclerosis, an 84-year-old woman, a 62-year-old man with a stroke, and a 36-year-old woman with schizophrenia).[8,9] The primary antibodies used were those against TGF-β1 (1:50, Santa Cruz), against versican (1:100, Seikagaku), and against the extra domain–A region of fibronectin (1:100, Abcam). The negative control was prepared with the use of nonimmune IgG as the primary antibody. We used cDNA encoding the extra domain–A region of fibronectin (spanning nucleotides 5404 through 5704 of fibronectin isoform 1 [region NM_212482.1]) as a template for digoxigenin-labeled antisense and sense-complementary RNA probes. The sense probe was used as a negative control. We carried out in situ hybridization on the paraffin-embedded sections by using the probes. After the sections had been washed and blocked, they were incubated with alkaline phosphatase–conjugated anti-digoxigenin antibodies, stained with 4-nitro-blue tetrazolium chloride–5-bromo-4-chloro-3-indolyl phosphate solution (Roche), and counterstained with fast red.

RESULTS

SUBJECTS

Clinical characteristics of the six probands with CARASIL are listed in Table 1, and the pedigrees are shown in Figure 1A. The patients in Families

Figure 1 (facing page). *HTRA1* Mutations in Families with Cerebral Autosomal Recessive Arteriopathy with Subcortical Infarcts and Leukoencephalopathy (CARASIL).

Panel A shows the pedigrees of families with CARASIL. Squares denote men; circles, women; solid symbols, affected family members; open symbols, unaffected members; and double horizontal lines, consanguineous marriage. Pairs of alleles of selected family members are listed for several microsatellite markers; the alleles are identified with the use of identification numbers 1 through 8. Genotypes whose haplotypic phases are unknown are shown in parentheses. Regions of homozygosity are delineated in boxes. Panel B shows the physical map of the candidate region for CARASIL on chromosome 10q. In Panels A and B, the microsatellite markers are listed in order from the centromere to the q-arm terminus; the candidate gene and the nucleotide mutations therein, carried by the probands, are indicated in red. Panel C shows the distribution of mutations in *HTRA1*, which consists of nine exons (squares): those encoding the insulin-like growth factor binding protein domain (green), the Kazal-type serine protease inhibitor domain (red), the trypsin-like serine protease domain (blue), and the PDZ domain (yellow), as well as untranslated regions (gray). Nucleotide (and corresponding amino acid) mutations are listed — missense in black and nonsense in red. Panel D shows the conservation of mutated HTRA1 amino acid residues in patients with CARASIL and in nonhuman species. Conserved residues are shaded (black, 100% conserved; dark gray, 80% conserved; gray, 60% conserved). The T at position 252 and the M at position 297 are highlighted in red; mutations at these positions are either completely or largely conserved. Sequences were obtained from GenBank. The results of magnetic resonance imaging (MRI) in patients with CARASIL are shown in Panels E, F, and G. Panels E and F show T_2-weighted images of the brain of Subject II-7, Family 3 (repetition time, 5000 msec; echo time, 150 msec; section thickness, 5 mm), revealing an ischemic region in the basal ganglia and white matter. T_1-weighted lumbar MRI (repetition time, 519 msec; echo time, 19 msec; section thickness, 5 mm) revealed spondylotic changes of the lumbar spine in Subject II-3, Family 2 (Panel G). Diffuse hair loss in the temporal and parietal areas of the head was observed in Subject II-2, Family 1 (Panel H) at 48 years of age. Cerebral small arteries in the arachnoid mater from Subject II-1, Family 6, show marked intimal thickening, narrowing of the lumen, hyalinosis, and splitting of the internal elastic membrane (Panel I, elastic van Gieson stain; scale bar, 1 mm).

1 through 5 were enrolled initially, and the causative gene for CARASIL was identified. We then enrolled an additional subject with pathologically confirmed CARASIL, in a sixth family, to perform immunohistochemical analysis. On neuropathological examination of this additional subject, arteriosclerosis associated with intimal thickening and dense collagen fibers were observed in cerebral small arteries (Fig. 1I).

The probands from the first five families had diffuse white-matter lesions on magnetic resonance imaging (MRI), autosomal recessive inheritance, an onset of initial symptoms between the second and fifth decade, and spondylosis or alopecia (Table 1 and Fig. 1E through 1H).[6-8] Although the affected persons in Family 5 did not have alopecia and cognitive impairment, we enrolled them because they had diffuse white-

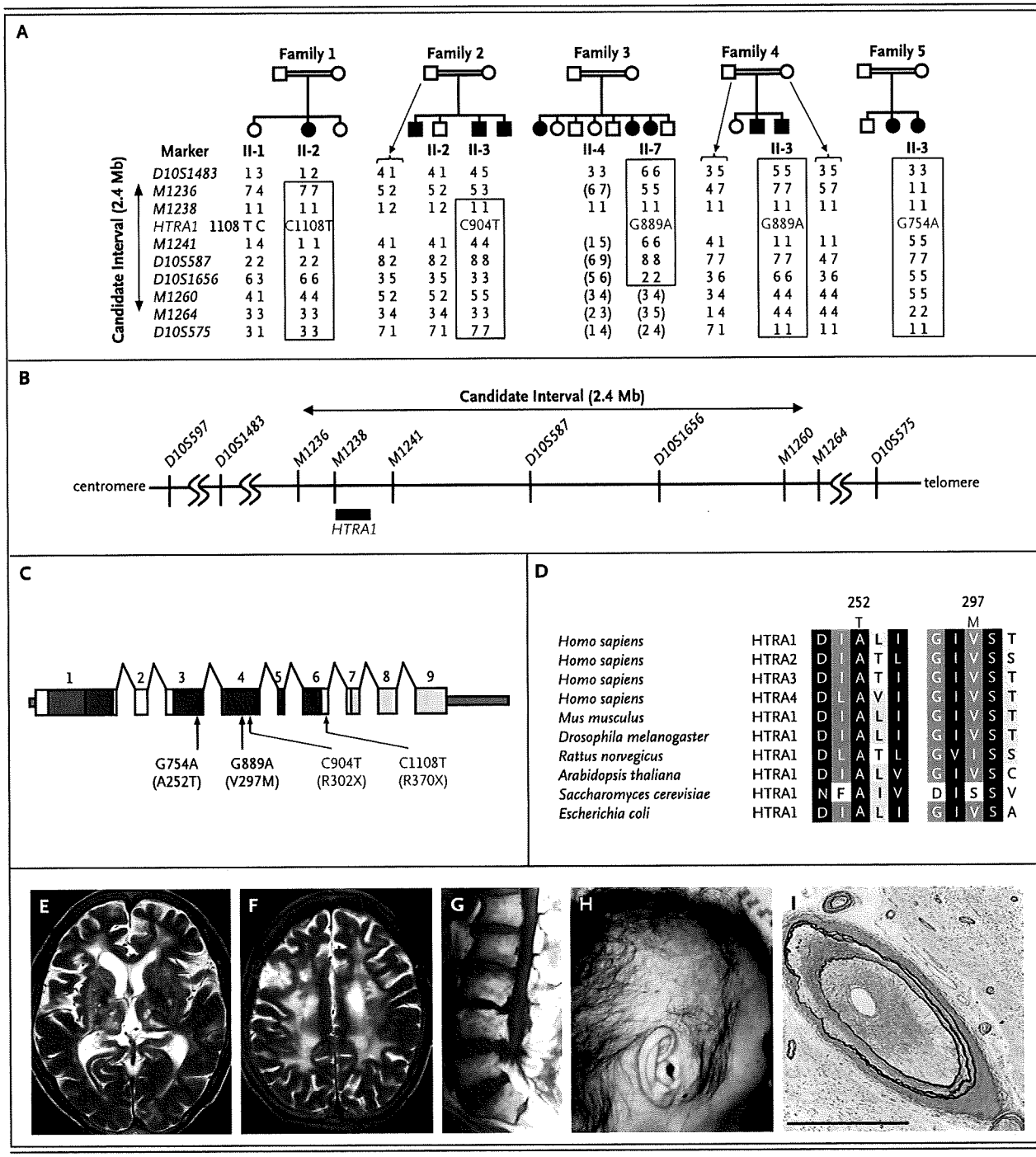

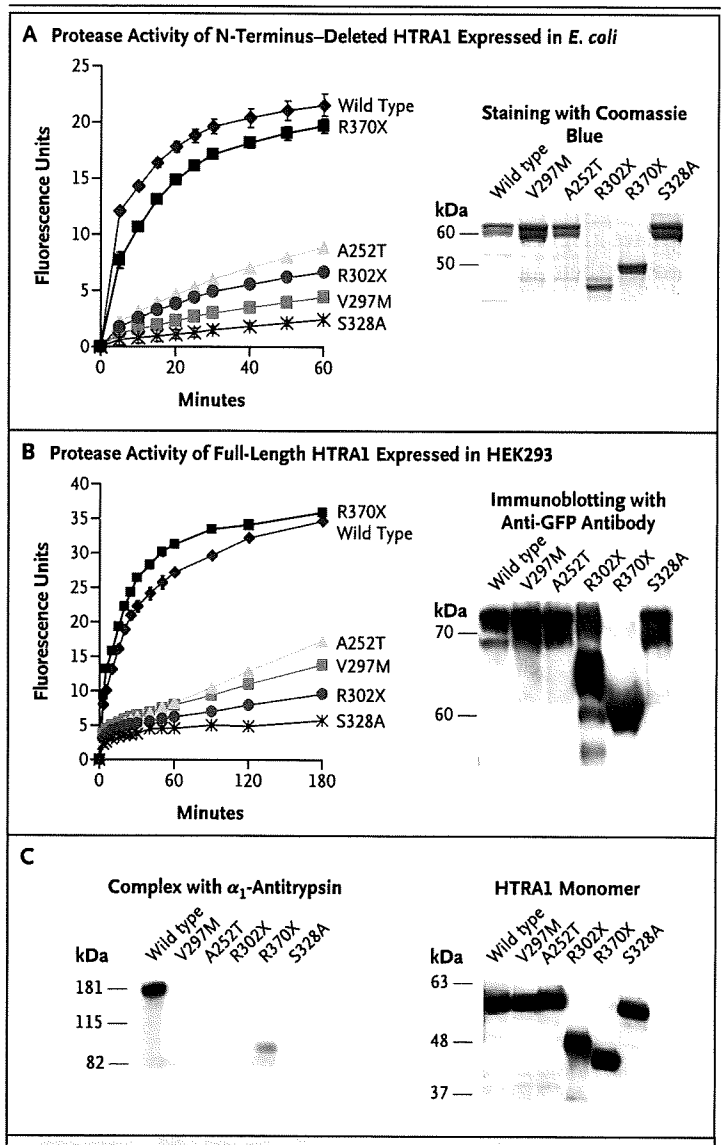

Figure 2. Functional Consequences of HTRA1 Mutations.

Panels A and B show the results of an assay with fluorescein isothiocyanate (FITC)–labeled β-casein. The fluorescence units represent protease activity. FITC-labeled β-casein was incubated with recombinant HTRA1 proteins in which the N-terminus has been deleted, expressed in *Escherichia coli* (Panel A), or serum-free medium containing cells from the human embryonic kidney cell line HEK293 that stably expressed HTRA1 tagged with a green fluorescent protein (GFP) at the C-terminus (Panel B). The quantity of HTRA1 protein was measured through staining with Coomassie blue (Panel A); the quality of the samples was ensured through immunoblotting with an anti-GFP antibody (Panel B). In Panels A and B, the I bars represent standard errors. Amino acid substitution of the serine protease motif S328A, which abolishes the protease activity in HTRA1, was used as a negative control.[14] Panel C (left) shows the formation of covalent complexes (high-molecular-weight products) between α_1-antitrypsin and wild-type or R370X HTRA1. The HTRA1 protein level was measured through immunoblotting with an anti–simian virus 5 antibody (right).

matter lesions on MRI and spondylosis, and one (a sibling of the proband in this family) had pathological findings identical to those in the patients with CARASIL.[8]

GENETIC ANALYSIS

From genomewide linkage analysis of the five families enrolled, we obtained maximal cumulative pairwise lod scores of 3.97 and 3.59 at *D10S587* and *D10S1656* (θ=0.0); all patients were homozygous for these loci (Fig. 1A). We then performed fine mapping of the region between *D10S597* and *D10S575* using *D10S1483* and five established polymorphic microsatellite markers (*M1236*, *M1238*, *M1241*, *M1260*, and *M1264*; see the Supplementary Appendix) (Fig. 1A and 1B). All probands were homozygous for the loci between *M1238* and *D10S1656*, suggesting that the causative gene was located within this 2.4-Mb region.

We first selected *HTRA1* as a candidate gene (Fig. 1B) because it is expressed in the blood vessels, skin, and bone.[19] We identified two homozygous nonsense nucleotide mutations: 1108C→T (resulting in a stop codon at position 370; amino acid mutation R370X) in Family 1 and 904C→T (resulting in a stop codon at 302; R302X) in Family 2 (Fig. 1C). We also identified two homozygous missense mutations: 889G→A (predicted to result in the amino acid substitution V297M) in Families 3 and 4 and 754G→A (predicted to result in the amino acid substitution A252T) in Family 5. In addition, we observed the homozygous nonsense mutation 904C→T again in the proband of Family 6. The missense mutations V297M and A252T were located in the genic region encoding the serine protease domain (Fig. 1C), and the amino acids predicted to be affected were either completely or largely conserved among the HTRA homologues HTRA1 through HTRA4 and among HTRA1 orthologues (Fig. 1D). We did not find evidence of such mutations in the 125 controls.

PROTEASE ACTIVITY OF MUTANT HTRA1

The level of protease activity in the mutant HTRA1 encoded by cDNA containing V297M, A252T, or R302X was 21% to 50% of the activity level in wild-type HTRA1. In contrast, HTRA1 encoded by a construct containing the R370X mutation had a protease activity level similar to that in wild-type HTRA1 (Fig. 2A and 2B). HTRA1 attacks the reactive center loop of α_1-antitrypsin, instigating

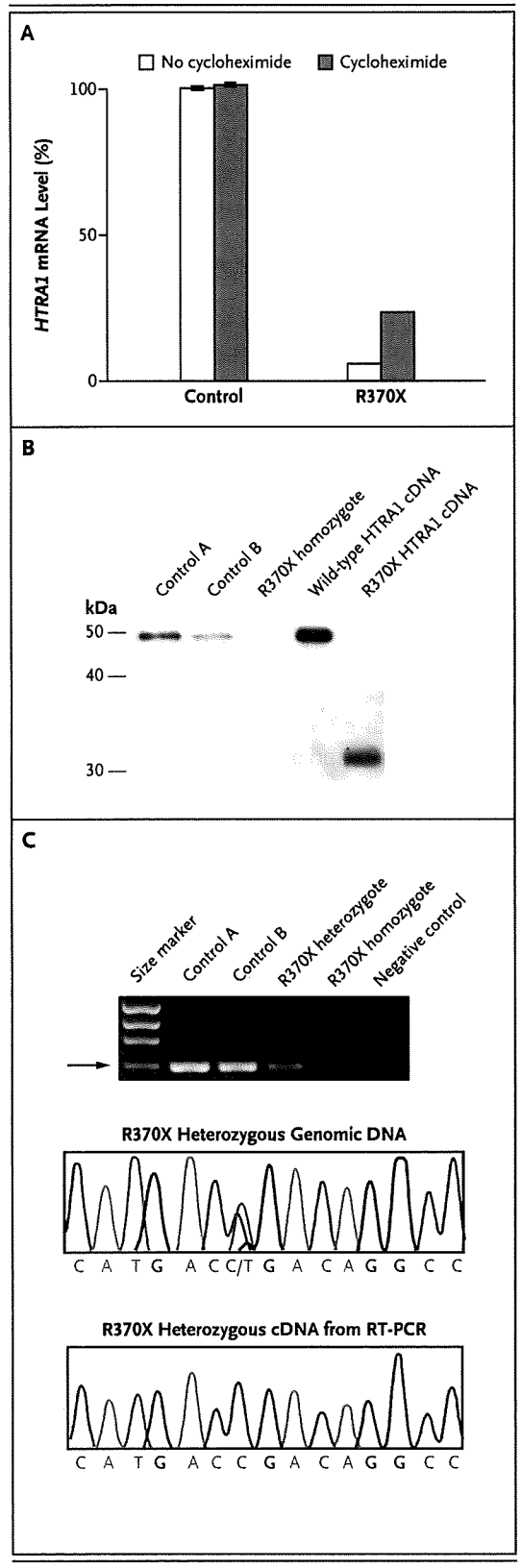

Figure 3. Nonsense-Mediated Decay of Mutant *HTRA1* Messenger RNA.

Panel A shows *HTRA1* messenger RNA (mRNA) levels in cultured skin fibroblasts from Subject II-2, Family 1, who is a homozygous carrier of R370X HTRA1, as a percentage of the average level of *HTRA1* mRNA in cells among four controls, with or without treatment with cycloheximide (100 μg per milliliter), an inhibitor of nonsense-mediated decay, for 4 hours. The I bars represent the standard errors. Panel B shows results of Western blotting of cultured skin fibroblasts obtained from Subject II-2, Family 1, the homozygous carrier of R370X, and two controls (A and B) with the use of an anti-HTRA1 antibody (MAB2916, R&D Systems). Wild-type and R370X complementary DNA (cDNA) was also assayed, for reference. Panel C shows the results of a reverse-transcriptase–polymerase-chain-reaction (RT-PCR) assay with the use of primers specific to the *HTRA1* sequence. We found PCR amplicons of the expected size (600 bp, arrow) with cDNA prepared from peripheral blood of Subject II-1, Family 1, an unaffected heterozygous carrier of R370X, but not with cDNA from Subject II-2, Family 1, the R370X homozygote. The negative control was a sample obtained from the heterozygous Subject II-1 that did not undergo reverse transcription. The electropherograms show wild-type and mutant (1108C→T) products derived from the genomic DNA of leukocytes from the heterozygous Subject II-1, whereas a wild-type allele only was detected in the RT-PCR products derived from the RNA of the leukocytes from the same subject.

the serine protease activity of α_1-antitrypsin, which thereby mediates the formation of a covalent complex between the two molecules.[14] We did not observe the formation of a stable complex between α_1-antitrypsin and mutant HTRA1 encoded by cDNA containing V297M, A252T, or R302X. In contrast, wild-type HTRA1 and HTRA1 encoded by cDNA containing R370X did form stable complexes with α_1-antitrypsin (Fig. 2C).

NONSENSE-MEDIATED DECAY

If a premature stop codon is located at least 50 to 55 nucleotides upstream of the exon–exon junction close to the 3′ end, mRNA may become degraded through nonsense-mediated decay.[20] Because the location of R370X fulfills this criterion for decay (Fig. 1C), we determined whether R370X-containing *HTRA1* mRNA is degraded by means of nonsense-mediated decay. The level of *HTRA1* mRNA expression in fibroblasts from the patient with the R370X mutation was 6.0% of that in fibroblasts from control subjects, and treatment with cycloheximide, an inhibitor of nonsense-mediated decay, increased this level by a factor of

four (Fig. 3A). We did not detect HTRA1 protein in the culture medium of fibroblasts from the patient carrying the R370X mutation (Subject II-2, Family 1) (Fig. 3B). Furthermore, analysis of *HTRA1* in leukocytes from a heterozygous carrier of this mutation (Subject II-1, Family 1) showed the presence of wild-type *HTRA1* mRNA only (Fig. 3C).

MUTANT HTRA1 AND SIGNALING BY TGF-β HOMOLOGUES

The serine protease activity of HTRA1 is necessary for inhibition of TGF-β family signaling.[16] We therefore tested the ability of mutant variants of HTRA1 with missense amino acids (i.e., A252T and V297M) to repress signaling by the TGF-β family members BMP-4 and BMP-2 (Fig. 4A, and Fig. 1 in the Supplementary Appendix). As expected, neither of the missense-mutated HTRA1 proteins repressed signaling by these molecules. To further investigate the ability of the mutant variants of HTRA1 to repress signaling by the TGF-β family members, we assayed phosphorylation of SMAD in these assays (phosphorylated SMAD is a downstream effector of the TGF-β–family signaling pathway), and observed that none of the mutant HTRA1 proteins repressed the subsequent phosphorylation of SMAD proteins (Fig. 4B, and Fig. 2 in the Supplementary Appendix).

We next investigated TGF-β signaling in fibroblasts from the subject with CARASIL carrying the R370X mutation and observed that TGF-β signaling in these fibroblasts was more than three times that in fibroblasts from control subjects (Fig. 4C). In addition, *NOG* mRNA, which is induced by TGF-β signaling in fibroblasts, was elevated in the proband (Fig. 4D, and Fig. 3 in the Supplementary Appendix).[21]

Increased TGF-β signaling results in vascular fibrosis, with synthesis of extracellular matrix proteins, including the extra domain–A region of fibronectin and versican.[22-24] In the patients with CARASIL who carried the R302X or A252T mutation, the tunica intima showed increased expression of the extra domain–A region of fibronectin (Fig. 4E through 4H, and Fig. 4A in the Supplementary Appendix) and versican (Fig. 4K, and Fig. 4B in the Supplementary Appendix), as compared with that in control subjects (Fig. 4M, 4N, and 4O). The result was confirmed by an in situ hybridization assay that used a probe for the extra domain–A region of fibronectin (Fig. 4I and

Figure 4 (facing page). Effect of Mutations on Transcription by Members of the Transforming Growth Factor β (TGF-β) Family.

Panel A shows the results of cotransfection of mouse C2C12 myoblasts with the pRL-TK renilla luciferase expression plasmid, the wild-type or a mutated HTRA1 expression plasmid, and other vector constructs designed to assay transcription by TGF-β1, bone morphogenetic protein (BMP-4 or BMP-2). Data are the means (from three independent experiments) of firefly luciferase activity, divided by the renilla luciferase activity, shown as the factor increase over the mean level among controls (negative for HTRA1 and TGF-β1). Panel B shows the results of cotransfection of the human embryonic kidney cell line HEK293 with the wild-type or a mutated HTRA1–simian virus 5 expression vector and other vector constructs designed to assay transcription by pro–TGF-β1, pro–BMP-4, or pro–BMP-2. Whole-cell lysates were immunoblotted. The data are the mean ratios of the expression levels of phosphorylated SMAD (pSMAD) and SMAD, among four independent experiments, shown as the factor increase over the mean ratio among controls (negative for HTRA1 and TGF-β1). The mean values for wild-type HTRA1 were significantly lower than those of the mutant HTRA1 ($P<0.05$ for all comparisons, by Tukey's multiple-comparison test). Amino acid substitution of the serine protease motif S328A, which abolishes the protease activity in HTRA1, was used as a negative control.[14] In Panel C, fibroblasts from two controls (A and B) and a homozygous carrier of R370X HTRA1 (Subject II-2, Family 1) were cotransfected with the pRL-TK renilla luciferase expression plasmid and vectors designed to assay transcription by TGF-β. Data are the means (from three independent experiments) of firefly luciferase activity, divided by the renilla luciferase activity, shown as the factor increase over the mean level among negative controls containing a reporter vector only (not shown). The mean values for the R370X cells are significantly higher than those in either control ($P<0.05$ for both comparisons, by Tukey's multiple-comparison test). Panel D shows noggin gene (*NOG*) messenger RNA (mRNA) levels (among three independent experiments for each subject) in fibroblasts from four controls and from the homozygous carrier of R370X HTRA1 (Subject II-2, Family 1). The expression level for Subject II-2 is shown as a ratio of the mean level in fibroblasts from four controls. In Panels A through D, the T bars indicate standard errors. Panels E through L show images of small cerebral arteries, obtained on autopsy, from Subject II-1, Family 6, who was homozygous for the R302X mutation. There was marked intimal proliferation (Panels E and G), increased expression of an extra domain–A region of fibronectin in the tunica intima (Panels F and H), increased mRNA expression of an extra domain–A region of fibronectin in endothelial cells (Panels I and J) and subendothelial smooth-muscle cells (Panel I), and increased expression of a versican in the tunica intima (Panel K) and TGF-β1 in the tunica media (Panel L). For comparison, Panels M, N, and P show images from immunohistochemical analysis of small cerebral arteries, obtained on autopsy, from a control (a 40-year-old woman with amyotrophic lateral sclerosis). The same results were obtained for three additional controls (an 84-year-old woman, a 62-year-old man with a stroke, and a 36-year-old woman with schizophrenia). Staining was performed with the elastic van Gieson stain in Panels E, G, and M; the anti–extra domain–A fibronectin antibody IST-9 in Panels F, H, and N; antisense probe for extra domain–A fibronectin in Panels I and J; antiversican antibody in Panels K and O; and anti–TGF-β1 antibody in Panels L and P. The scale bars in Panels E through P indicate 100 μm.

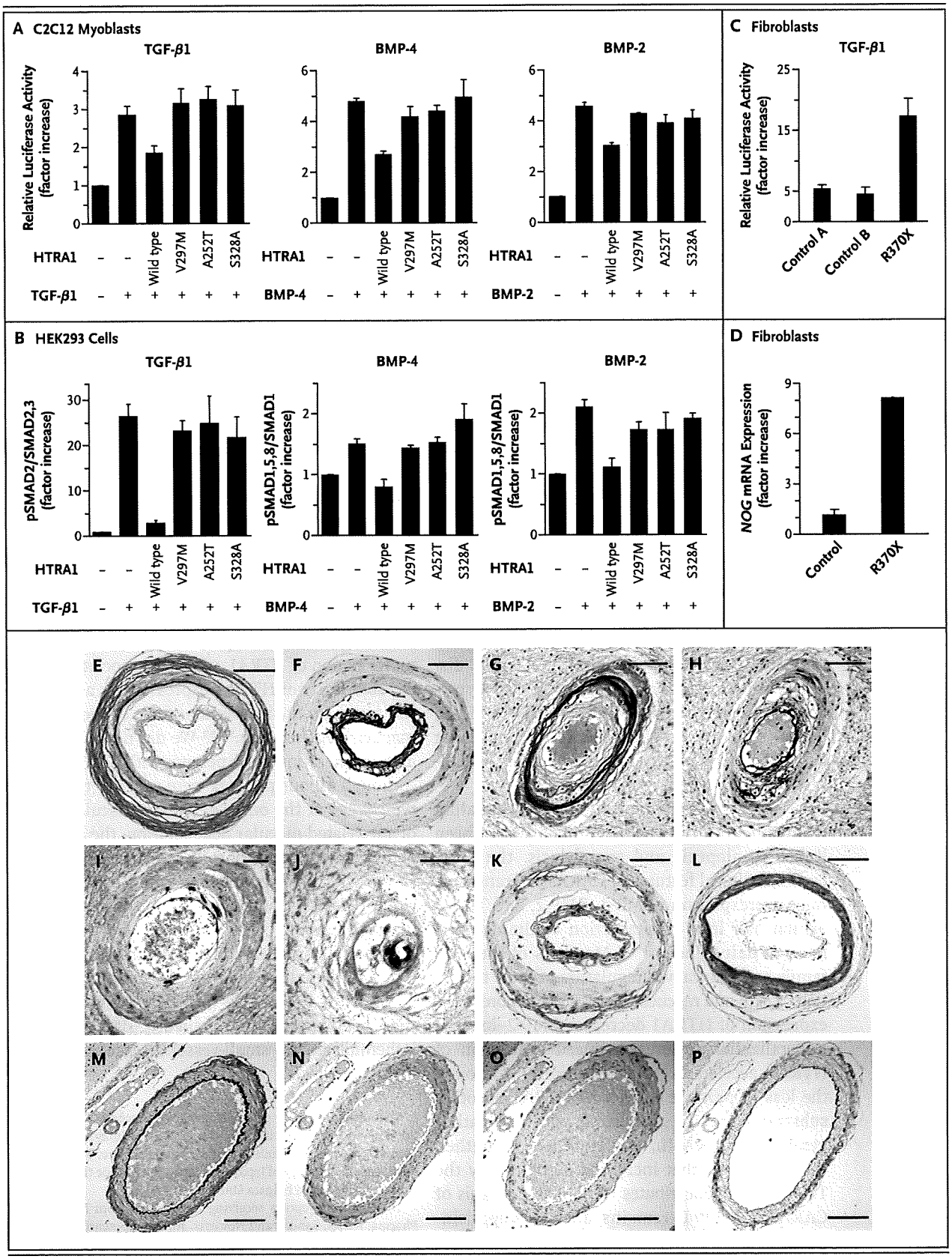

4J, and Fig. 5 in the Supplementary Appendix). Moreover, in the patients with CARASIL, the tunica media exhibited elevated expression of TGF-β1 (Fig. 4L and 4P, and Fig. 4C in the Supplementary Appendix). These results indicate increased TGF-β signaling in the cerebral small arteries in patients with CARASIL.

DISCUSSION

Signaling by members of the TGF-β family is closely associated with vascular angiogenesis and remodeling and has multifaceted roles in vascular endothelial and smooth-muscle cells, depending on the type of cell and extracellular matrix.[25,26] Moreover, dysregulation of TGF-β–family signaling results in hereditary vascular disorders.[26] Defective TGF-β signaling due to mutations in the TGF-β receptors leads to hereditary hemorrhagic telangiectasia, whereas activation of TGF-β signaling contributes to Marfan's syndrome and associated disorders.[26] Our findings extend the spectrum of diseases associated with the dysregulation of TGF-β signaling to include hereditary ischemic cerebral small-vessel disease. In addition, the pathological findings in patients with CARASIL resemble those observed in patients with nonhereditary ischemic cerebral small-vessel disease with hypertension, suggesting that hypertension may increase TGF-β signaling.[7-11,27] Thus, TGF-β signaling might underlie the molecular basis of nonhereditary ischemic cerebral small-vessel disease with hypertension.

Dysregulation of the inhibition of signaling by members of the TGF-β family also has been linked to alopecia and spondylosis, the other cardinal clinical features of CARASIL. Transgenic mice overexpressing BMP-4, BMP-2, and TGF-β exhibit hair loss or retardation of the development of hair follicles.[28,29] Members of the BMP family are well-known regulators of bone formation, repair, and regeneration.[30] Furthermore, overexpression of HTRA1 decreases BMP-2–induced mineralization, whereas reduced expression of HTRA1 accelerates mineralization.[31] Although the loss of protease activity by HTRA1 on other substrates may be associated with the pathogenesis of CARASIL, our findings strengthen the hypothesis that increased signaling by the TGF-β family contributes to the pathogenesis of CARASIL.[14,31-33] It remains unclear why disinhibition of signaling by TGF-β family members caused by mutant HTRA1 results in narrowly restricted clinical phenotypes. Possible explanations are tissue-specific regulation of signaling by the TGF-β family and tissue-specific expression of HTRA1.[14,19,33,34]

The molecular basis for regulation of TGF-β1 signaling by HTRA1 remains to be elucidated.[16,35,36] TGF-β1 is synthesized as a proprotein (pro–TGF-β1) and is subsequently cleaved into latency-associated protein and mature TGF-β1 by proprotein convertase.[26] The mature TGF-β1 is noncovalently bound to the latency-associated protein and is sequestered as a latency-associated protein–TGF-β1 complex in an extracellular matrix.[26] The mature TGF-β1 is released from the latency-associated protein–TGF-β1 complex. Therefore, the TGF-β1 signaling is regulated by a balance among maturation, sequestration, and presentation. The elastin microfibril interfacer 1 protein (EMILIN1) inhibits TGF-β1 signaling by preventing the processing of pro–TGF-β1 into mature TGF-β1.[37] In our study, the patients with CARASIL had increased expression of mature TGF-β1, suggesting that the HTRA1 may also prevent the processing of pro–TGF-β1 into mature TGF-β1, depending on its protease activity.

A single-nucleotide polymorphism in the promoter region of *HTRA1*, which is associated with elevated levels of HTRA1 expression, is a genetic risk factor for the neovascular form of age-related macular degeneration.[38,39] We did not find macular degeneration in the persons with CARASIL.[6-8] Although all our patients were younger than the typical age at the onset of the neovascular form of age-related macular degeneration, the absence of macular degeneration in the patients is consistent with the hypothesis that increased expression of HTRA1 contributes to age-related macular degeneration.[6-8,38]

Our results indicate that disinhibition of TGF-β–family signaling underlies the molecular basis of CARASIL. They also provide a basis for further investigation of therapeutic strategies for ischemic cerebral small-vessel disease, alopecia, and spondylosis.

Supported in part by grants from the Advanced Brain Science Project and Applied Genomics, the Center for Integrated Brain Medical Science, the Ministry of Education, Culture, Sports, Science, and Technology of Japan, the Japan Society for the Promotion of Science, and Niigata University.

Dr. Fukutake reports receiving lecture fees from Mitsubishi Pharma, Kissei, Sanofi, and Novartis. No other potential conflict of interest relevant to this article was reported.

We thank the patients and family members for their participation; M. Tsuchiya, Y. Hazama, Y. Koike, R. Izumita, and M. Nihonmatsu for technical assistance; and Drs. B. Vogelstein (Howard Hughes Medical Institute and Sidney Kimmel Comprehensive Cancer Center), T. Katagiri (Saitama Medical School Research Center for Genomic Medicine), and E. Schwartz (Institut für Biotechnologie, Martin Luther Universität Halle–Wittenberg) for their generous gifts of plasmids.

REFERENCES

1. Chui HC. Subcortical ischemic vascular dementia. Neurol Clin 2007;25:717-40.
2. Joutel A, Corpechot C, Ducros A, et al. Notch3 mutations in CADASIL, a hereditary adult-onset condition causing stroke and dementia. Nature 1996;383:707-10.
3. Richards A, van den Maagdenberg AM, Jen JC, et al. C-terminal truncations in human 3′-5′ DNA exonuclease TREX1 cause autosomal dominant retinal vasculopathy with cerebral leukodystrophy. Nat Genet 2007;39:1068-70.
4. Gould DB, Phalan FC, van Mil SE, et al. Role of COL4A1 in small-vessel disease and hemorrhagic stroke. N Engl J Med 2006;354:1489-96.
5. Revesz T, Ghiso J, Lashley T, et al. Cerebral amyloid angiopathies: a pathologic, biochemical, and genetic view. J Neuropathol Exp Neurol 2003;62:885-98.
6. Fukutake T, Hirayama K. Familial young-adult-onset arteriosclerotic leukoencephalopathy with alopecia and lumbago without arterial hypertension. Eur Neurol 1995;35:69-79.
7. Maeda S, Nakayama H, Isaka K, Aihara Y, Nemoto S. Familial unusual encephalopathy of Binswanger's type without hypertension. Folia Psychiatr Neurol Jpn 1976;30:165-77.
8. Yanagawa S, Ito N, Arima K, Ikeda S. Cerebral autosomal recessive arteriopathy with subcortical infarcts and leukoencephalopathy. Neurology 2002;58:817-20.
9. Oide T, Nakayama H, Yanagawa S, Ito N, Ikeda S, Arima K. Extensive loss of arterial medial smooth muscle cells and mural extracellular matrix in cerebral autosomal recessive arteriopathy with subcortical infarcts and leukoencephalopathy (CARASIL). Neuropathology 2008;28:132-42.
10. Okeda R, Murayama S, Sawabe M, Kuroiwa T. Pathology of the cerebral artery in Binswanger's disease in the aged: observation by serial sections and morphometry of the cerebral arteries. Neuropathology 2004;24:21-9.
11. Tanoi Y, Okeda R, Budka H. Binswanger's encephalopathy: serial sections and morphometry of the cerebral arteries. Acta Neuropathol 2000;100:347-55.
12. Lathrop GM, Lalouel JM, Julier C, Ott J. Strategies for multilocus linkage analysis in humans. Proc Natl Acad Sci U S A 1984; 81:3443-6.
13. Cottingham RW Jr, Idury RM, Schäffer AA. Faster sequential genetic linkage computations. Am J Hum Genet 1993;53:252-63.
14. Hu SI, Carozza M, Klein M, Nantermet P, Luk D, Crowl RM. Human HtrA, an evolutionarily conserved serine protease identified as a differentially expressed gene product in osteoarthritic cartilage. J Biol Chem 1998;273:34406-12.
15. Brunner AM, Marquardt H, Malacko AR, Lioubin MN, Purchio AF. Site-directed mutagenesis of cysteine residues in the pro region of the transforming growth factor β 1 precursor: expression and characterization of mutant proteins. J Biol Chem 1989;264:13660-4.
16. Oka C, Tsujimoto R, Kajikawa M, et al. HtrA1 serine protease inhibits signaling mediated by Tgfβ family proteins. Development 2004;131:1041-53.
17. Katagiri T, Imada M, Yanai T, Suda T, Takahashi N, Kamijo R. Identification of a BMP-responsive element in Id1, the gene for inhibition of myogenesis. Genes Cells 2002;7:949-60.
18. Hillger F, Herr G, Rudolph R, Schwarz E. Biophysical comparison of BMP-2, ProBMP-2, and the free pro-peptide reveals stabilization of the pro-peptide by the mature growth factor. J Biol Chem 2005;280:14974-80.
19. De Luca A, De Falco M, Severino A, et al. Distribution of the serine protease HtrA1 in normal human tissues. J Histochem Cytochem 2003;51:1279-84.
20. Kuzmiak HA, Maquat LE. Applying nonsense-mediated mRNA decay research to the clinic: progress and challenges. Trends Mol Med 2006;12:306-16.
21. Gazzerro E, Gangji V, Canalis E. Bone morphogenetic proteins induce the expression of noggin, which limits their activity in cultured rat osteoblasts. J Clin Invest 1998;102:2106-14.
22. Glukhova MA, Frid MG, Shekhonin BV, et al. Expression of extra domain A fibronectin sequence in vascular smooth muscle cells is phenotype dependent. J Cell Biol 1989;109:357-66.
23. Leask A, Abraham DJ. TGF-β signaling and the fibrotic response. FASEB J 2004;18:816-27.
24. Schönherr E, Järveläinen HT, Sandell LJ, Wight TN. Effects of platelet-derived growth factor and transforming growth factor-β 1 on the synthesis of a large versican-like chondroitin sulfate proteoglycan by arterial smooth muscle cells. J Biol Chem 1991;266:17640-7.
25. Grainger DJ. Transforming growth factor β and atherosclerosis: so far, so good for the protective cytokine hypothesis. Arterioscler Thromb Vasc Biol 2004; 24:399-404.
26. ten Dijke P, Arthur HM. Extracellular control of TGFβ signalling in vascular development and disease. Nat Rev Mol Cell Biol 2007;8:857-69.
27. O'Callaghan CJ, Williams B. Mechanical strain-induced extracellular matrix production by human vascular smooth muscle cells: role of TGF-β(1). Hypertension 2000;36:319-24.
28. Liu X, Alexander V, Vijayachandra K, Bhogte E, Diamond I, Glick A. Conditional epidermal expression of TGFβ 1 blocks neonatal lethality but causes a reversible hyperplasia and alopecia. Proc Natl Acad Sci U S A 2001;98:9139-44.
29. Botchkarev VA. Bone morphogenetic proteins and their antagonists in skin and hair follicle biology. J Invest Dermatol 2003;120:36-47.
30. Yoon BS, Lyons KM. Multiple functions of BMPs in chondrogenesis. J Cell Biochem 2004;93:93-103.
31. Hadfield KD, Rock CF, Inkson CA, et al. HtrA1 inhibits mineral deposition by osteoblasts: requirement for the protease and PDZ domains. J Biol Chem 2008;283: 5928-38.
32. Clausen T, Southan C, Ehrmann M. The HtrA family of proteases: implications for protein composition and cell fate. Mol Cell 2002;10:443-55.
33. Tsuchiya A, Yano M, Tocharus J, et al. Expression of mouse HtrA1 serine protease in normal bone and cartilage and its upregulation in joint cartilage damaged by experimental arthritis. Bone 2005;37:323-36.
34. Grau S, Baldi A, Bussani R, et al. Implications of the serine protease HtrA1 in amyloid precursor protein processing. Proc Natl Acad Sci U S A 2005;102:6021-6.
35. Gilicze A, Kohalmi B, Pocza P, et al. HtrA1 is a novel mast cell serine protease of mice and men. Mol Immunol 2007;44: 2961-8.
36. Launay S, Maubert E, Lebeurrier N, et al. HtrA1-dependent proteolysis of TGF-β controls both neuronal maturation and developmental survival. Cell Death Differ 2008;15:1408-16.
37. Zacchigna L, Vecchione C, Notte A, et al. Emilin1 links TGF-β maturation to blood pressure homeostasis. Cell 2006; 124:929-42.
38. Dewan A, Liu M, Hartman S, et al. HTRA1 promoter polymorphism in wet age-related macular degeneration. Science 2006;314:989-92.
39. Yang Z, Camp NJ, Sun H, et al. A variant of the HTRA1 gene increases susceptibility to age-related macular degeneration. Science 2006;314:992-3.

Self-Contained Induction of Neurons from Human Embryonic Stem Cells

Tsuyoshi Okuno[1,2], Takashi Nakayama[3], Nae Konishi[1], Hideo Michibata[1], Koji Wakimoto[1], Yutaka Suzuki[1], Shinji Nito[1], Toshio Inaba[2], Imaharu Nakano[4], Shin-ichi Muramatsu[4], Makoto Takano[5], Yasushi Kondo[1]*, Nobuo Inoue[6]

1 Advanced Medical Research Laboratory, Mitsubishi Tanabe Pharma Corporation, Osaka, Japan, 2 Department of Advanced Pathobiology, Graduate School of Life and Environmental Sciences, Osaka Prefecture University, Osaka, Japan, 3 Department of Biochemistry, Yokohama City University School of Medicine, Yokohama, Japan, 4 Division of Neurology, Department of Medicine, Jichi Medical University, Tochigi, Japan, 5 Department of Physiology, Jichi Medical University, Tochigi, Japan, 6 Laboratory of Regenerative Neurosciences, Graduate School of Human Health Sciences, Tokyo Metropolitan University, Tokyo, Japan

Abstract

Background: Neurons and glial cells can be efficiently induced from mouse embryonic stem (ES) cells in a conditioned medium collected from rat primary-cultured astrocytes (P-ACM). However, the use of rodent primary cells for clinical applications may be hampered by limited supply and risk of contamination with xeno-proteins.

Methodology/Principal Findings: We have developed an alternative method for unimpeded production of human neurons under xeno-free conditions. Initially, neural stem cells in sphere-like clusters were induced from human ES (hES) cells after being cultured in P-ACM under free-floating conditions. The resultant neural stem cells could circumferentially proliferate under subsequent adhesive culture, and selectively differentiate into neurons or astrocytes by changing the medium to P-ACM or G5, respectively. These hES cell-derived neurons and astrocytes could procure functions similar to those of primary cells. Interestingly, a conditioned medium obtained from the hES cell-derived astrocytes (ES-ACM) could successfully be used to substitute P-ACM for induction of neurons. Neurons made by this method could survive in mice brain after xeno-transplantation.

Conclusion/Significance: By inducing astrocytes from hES cells in a chemically defined medium, we could produce human neurons without the use of P-ACM. This self-serving method provides an unlimited source of human neural cells and may facilitate clinical applications of hES cells for neurological diseases.

Citation: Okuno T, Nakayama T, Konishi N, Michibata H, Wakimoto K, et al. (2009) Self-Contained Induction of Neurons from Human Embryonic Stem Cells. PLoS ONE 4(7): e6318. doi:10.1371/journal.pone.0006318

Editor: Tailoi Chan-Ling, University of Sydney, Australia

Received June 3, 2008; **Accepted** June 24, 2009; **Published** July 21, 2009

Funding: Part of this work was supported by grants from the Ministry of Education, Science, Sports and Culture, the Japanese Government; and from the Japan Ministry of Health, Labor and Welfare.

Competing Interests: The authors have declared that no competing interests exist.

* E-mail: kondo.yasushi@mc.mt-pharma.co.jp

Introduction

Embryonic stem (ES) cells, derived from the inner cell mass of blastocysts, are pluripotent cells that can differentiate into a variety of cell types including neural cells [1,2]. Among the various basic and clinical applications for ES cells, cell transplantation therapy for central nervous diseases is of particular interest because differentiated neurons do not proliferate, and a relatively large number of donor cells are necessary to replace diseased neurons. Several methods have been developed to prepare neural cells from ES cells. Neurons can be obtained indirectly from ES cells via ectodermal cells in embryoid bodies, which are formed from dissociated ES cells, either by induction with retinoic acid or selection [3,4]. Alternatively, neural stem cells and neurons can be directly differentiated from ES cells without forming embryoid bodies by culturing ES cells on mouse-cultured stroma cells (PA-6) [5], or under chemically defined low-density culture conditions [6]. All of these procedures, however, are time consuming and require highly complicated processes to generate many neurons. In addition, their practicality is limited by the possible teratogenicity caused by culture factors, such as retinoic acid, of differentiated cells. We have previously reported an efficient method to prepare transplantable neural cells from mouse ES cells using a conditioned medium collected from rat primary-cultured astrocytes (P-ACM) [7–9]. In this study, we applied this method to human ES (hES) cells for induction of neurons and astrocytes. Once the astrocytes were derived from hES cells, they could be substituted for primary astrocytes that induce neurons, thus achieving xeno-free production of neurons.

Results

Neural cell differentiation from hES

Four hES cell-lines stably expressing humanized renilla green fluorescent protein (hrGFP) were obtained. These hES cell-lines were kept in undifferentiated state with positive stem cell markers, such as alkaline phosphatase, Oct-4, and SSEA-4. When cultured

in P-ACM containing fibroblast growth factor-2 (FGF-2) under free-floating conditions, colonies of undifferentiated hES cells gave rise to floating spheres composed of neural stem cells and undifferentiated cells, which gradually increased in size during the culture. After 12 days of culture, the spheres were plated onto a poly-L-Lysine/Laminin coated dish and cultivated in neural stem cell medium (NSCM) containing high concentrations of FGF-2 and epidermal growth factor (EGF). Within 24 h, the spheres attached onto the substrate and formed circular clusters of cells. Many of these cells subsequently migrated to the surrounding areas and covered the growth surface of the dish in circular monolayers. After replacing NSCM by P-ACM and culture for 14 days, the spheres differentiated into neurons (Figures 1A, B) and few astrocytes (Figures 1C). These were identified by the neuronal marker tubulin β III isoform (Tuj1) and the astrocytic marker glial fibrillary acidic protein (GFAP).

Selective differentiation of hES cells into neurons and astrocytes

By culture of the spheres in NSCM, neural stem cells were able to migrate from the attached spheres to the surrounding area and subsequently form a circular cluster. NSCM containing FGF-2 and EGF promotes neural stem cells proliferation, while repressing their differentiation into any type of neural cells. After removing the core of the attached spheres mechanically, the remaining neural stem cells could proliferate in NSCM and selectively differentiate into neurons and astrocytes by subculture in an appropriate medium. To differentiate into neurons, neural stem cells were subcultured using 0.05% Trypsin/EDTA in P-ACM for 14 days (Figures 2A, B). After these 14 days of subculture, a large number of cells expressed Tuj1 ($84.0 \pm 5.1\%$, $n = 3$). On the other hand, to differentiate into astrocytes, neural stem cells were subcultured in G5 medium for 14 days (Figure 2C). After this subculture, a large number of cells expressed

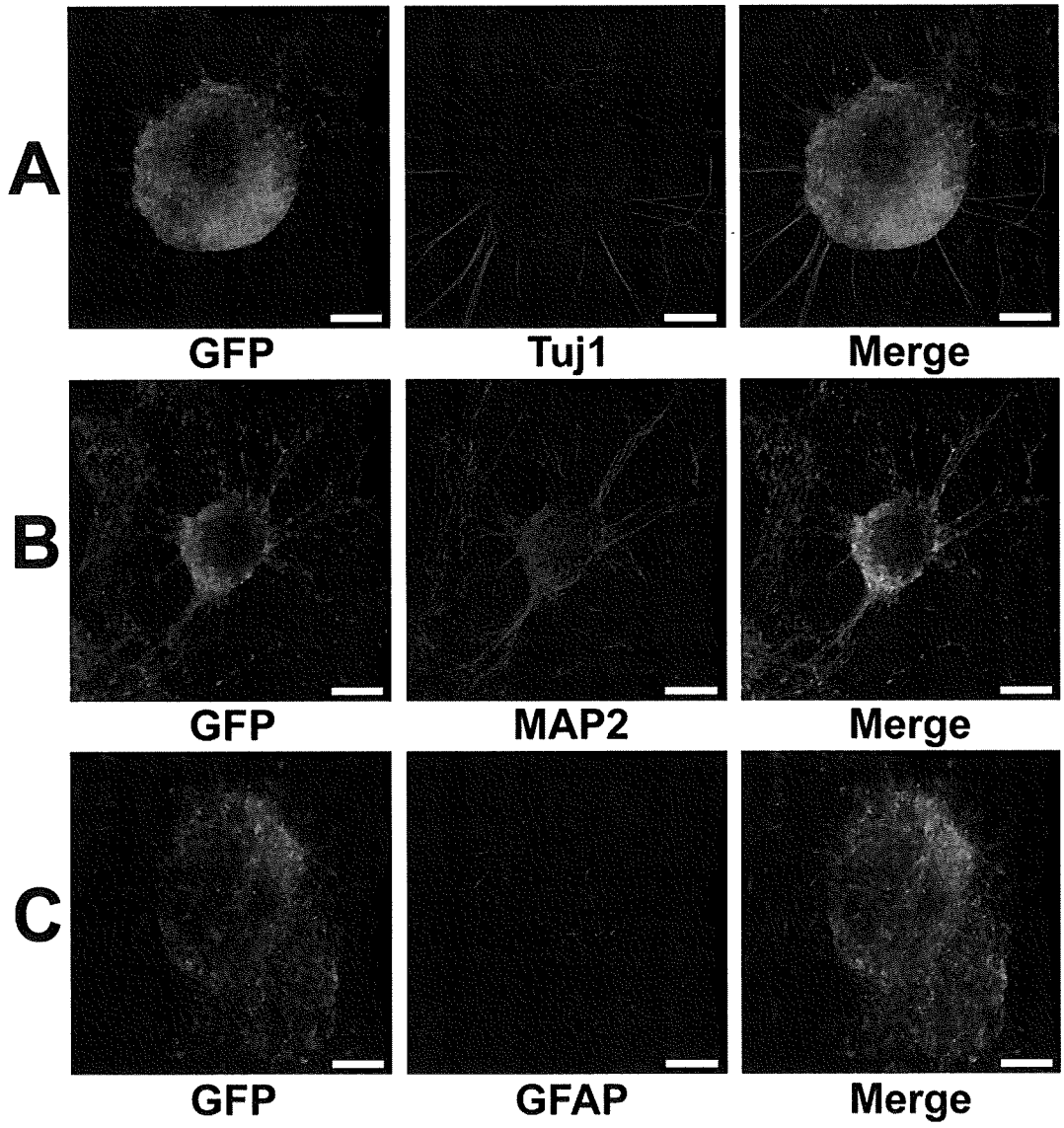

Figure 1. Differentiation of hES cells into neurons in P-ACM. Floating spheres composed of neural stem cells and undifferentiated cells grown for 12 days were plated on an adhesive substrate and cultured for 14 days in P-ACM. Expression of hrGFP (green), Tuj1 (A, red), MAP2 (B, red), and GFAP (C, red) staining of the many neural and few glial cells derived from hES cells. Bar = 100 μm.
doi:10.1371/journal.pone.0006318.g001

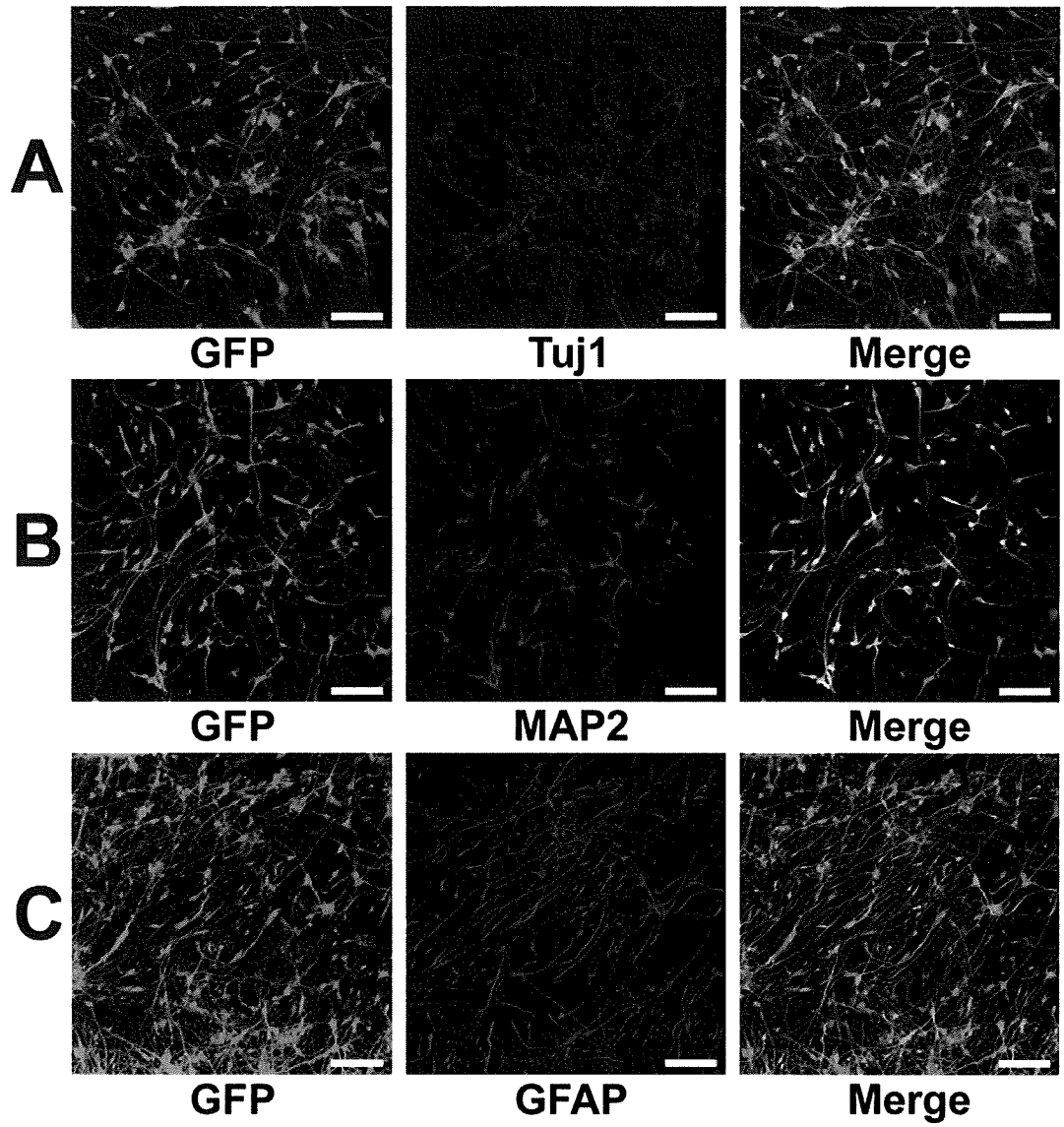

Figure 2. Selective induction of hES cells into neurons and astrocytes. (A, B): Neural stem cells that had migrated from floating spheres in NSCM were subcultured onto a PLL coated plate and cultured for 14 days in P-ACM. Immunostaining with antibody to Tuj1 and MAP2 showed that the subcultured neural stem cells had differentiated into neurons. Expression of hrGFP (green), (A) Tuj1 (red), and (B) MAP2 (red) staining profiles. (C): Neural stem cells were cultured for 14 days after removal of the core of spheres with a glass pipette and change of medium to G5 medium. The proliferated cells were subcultured onto PLL/LAM coated plate and cultured for 14 days in G5 medium. Immunostaining with antibody to GFAP showed that the subcultured cells had differentiated into astrocytes. Expression of hrGFP (green) and GFAP (red) staining profiles. Bar = 100 μm.
doi:10.1371/journal.pone.0006318.g002

GFAP (75.0±1.2%, $n = 3$). The removed core of the attached spheres could, like the first spheres, be used repeatedly (about twenty times) as seed for neural stem cells.

Xeno-free induction of astrocytes using a chemically defined medium

For collection of xeno-free astrocytes derived from hES cells, we used a chemically defined N2 medium for neural induction. When cultured in N2 medium containing FGF-2 and EGF under free-floating conditions, colonies of undifferentiated hES cells gave rise to floating spheres. As N2 was less efficient than P-ACM for obtaining astrocytes, we prepared hES cells in large scale ($>10^8$ cells). After differentiation, millions of astrocytes were gained under xeno-free condition (Figure 3A).

Neuronal induction of hES cell-derived astrocytes

Next, we investigated whether the astrocytes derived from hES cells can be substituted for primary astrocytes to differentiate hES cells into neural cells. A conditioned medium of hES cell-derived astrocytes was collected after two days culture and used as ES-ACM by adding an equal amount of N2 medium. As in the case of P-ACM, hES cells cultured in ES-ACM differentiated into neural cells via formation of spheres. After switching the cells from NSCM to ES-ACM, many cells had neuronal-like appearance with long neurites. By 6 weeks of culture in ES-ACM, most cells had neural morphology and expressed microtubule-associated protein 2 (MAP2) (Figure 3B). During our procedure for differentiating hES cells using ES-ACM, expression of several markers was analyzed by RT-PCR (Figure 4A). By 8 weeks culture

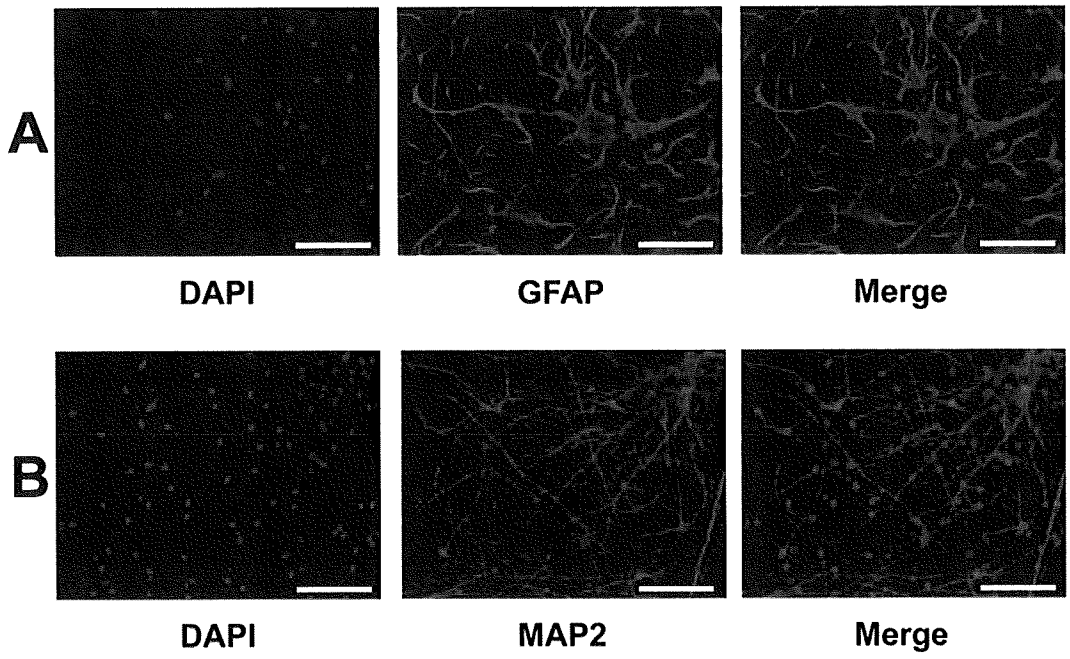

Figure 3. Differentiation of hES cells into astrocytes in a chemically defined medium. (A): Neural stem cells induced by N2 medium were cultured for 14 days after removal of the core of spheres with a glass pipette and change of medium to G5 medium. The proliferated cells were subcultured onto a PLL/LAM coated plate and cultured for 14 days in G5 medium. Immunostaining with antibody to GFAP showed that most of the subcultured cells had differentiated into astrocytes. DAPI (blue) and GFAP (green) staining profiles. Neural stem cells induced by xeno-free ES-ACM were subcultured onto PLL coated plate and cultured for 6 weeks in ES-ACM. (B): Immunostaining with antibody to MAP2 showed that the subcultured NSCs had differentiated into mature neurons. DAPI (blue) and MAP2 (red) staining profiles. Bar = 100 μm.
doi:10.1371/journal.pone.0006318.g003

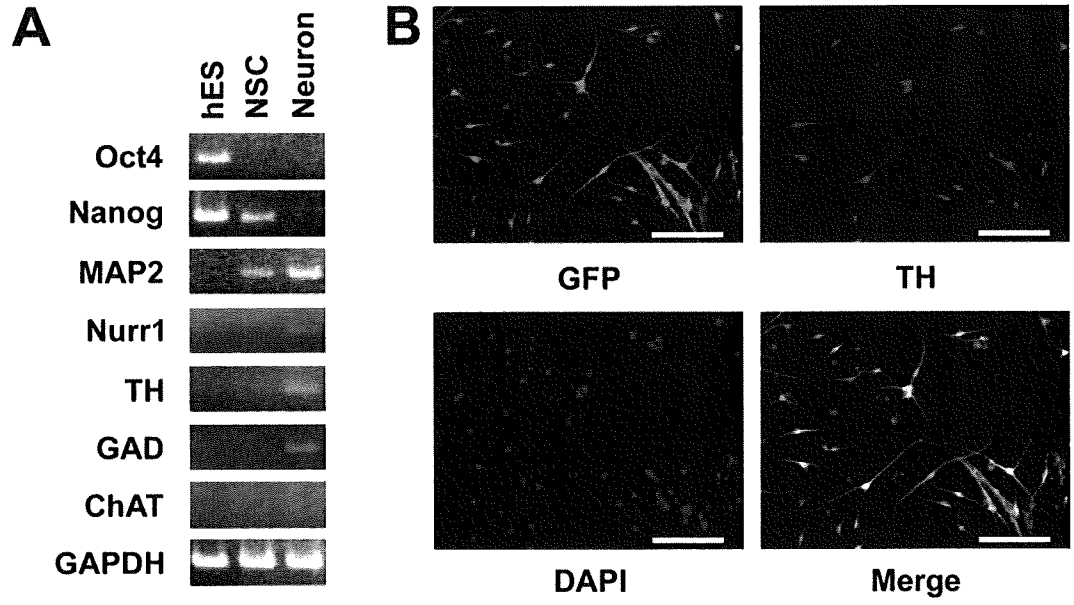

Figure 4. RT-PCR analysis and differentiation of hES cells into dopaminergic neurons in xeno-free ES-ACM. (A): RT-PCR analysis of hES cells, neural stem cells and mature neurons. RNA was isolated from clones of undifferentiated hES cells, from neural stem cells, and from mature neurons which had been cultured for 8 weeks in ES-ACM and analyzed for expression of marker genes. The expression levels of each gene were normalized to GAPDH gene expression level. hES, undifferentiated hES cells; NSC, neural stem cells; Neuron; mature neurons. (B): Differentiation of hES cells into dopaminergic neural cells in xeno-free ES-ACM. Neural stem cells induced by ES-ACM were subcultured onto PLL coated plate and cultured for 8 weeks in ES-ACM. Immunostaining with antibody TH and expression of hrGFP showed that the subcultured neural stem cells had differentiated into dopaminergic neurons. Expression of hrGFP (green), DAPI (blue) and TH (red) staining profiles. Bar = 100 μm.
doi:10.1371/journal.pone.0006318.g004

in ES-ACM, some cells showed tyrosine hydroxylase (TH) -immunoreactivity (Figure 4B). Furthermore, when cultured in ES-ACM again, the cells could differentiate into astrocytes via formation of spheres. To induce differentiation of neural stem cells into astrocytes, the culture medium was changed from NSCM to G5 medium. After medium change, most neural stem cells had the appearance of typical astrocytes. By 2 weeks culture in G5 medium, the majority (82.4±1.8%, $n=3$) of cells expressed GFAP, and few (<1%) expressed MAP2.

Electrophysiological analysis of neurons differentiated from hES cells

For electrophysiological study, hES-derived neurons were cultured on coverslips for 4–6 weeks. The coverslips were transferred to a recording chamber before use. Neurons were selected based on their appearance (spherical shape with long neurites). The resting membrane potential of the neurons were −62.0~−11.1 mV ($n=26$). Among 26 cells examined, action potentials were elicited in 22 cells (Figure 5A, Control). Application of 1 μM tetrodotoxin (TTX) completely suppressed the overshoot (Figure 5A, right panel). The action potentials were evoked only when resting membrane potentials were set to −70 mV by current injection in 11 cells. The rest of the cells did not possess membrane excitability ($n=4$ out of 26, closed circle in Figure 5B).

Survival of hES cell-derived neurons in mice brain

To examine differentiation of hES cell-derived cells *in vivo*, we transplanted neural stem cells induced with ES-ACM into mice brain ($n=7$). Before transplantation, the majority (85.1±5.1%, $n=4$) of donor cells expressed Nestin, a marker for neural stem cell (Figure 6A), and no cells expressed octamer transcription factor-3 (Oct-3) and stage-specific embryonic antigen (SSEA-4), two makers for undifferentiated cells (data not shown). Four weeks after engraftment, many ($2–3\times10^2$) hrGFP-positive cells were recognized (Figure 6B, C). Some of these cells (<10%) were also Tuj1-immunoreactive (Figure 6D). In the vicinity of the grafts, few cells were immunoreactive against Ki-67, a marker for proliferation. However, none of these Ki-67-positive cells were positive for hrGFP (Figure 6E). Teratoma was not detected in any of the transplanted mice.

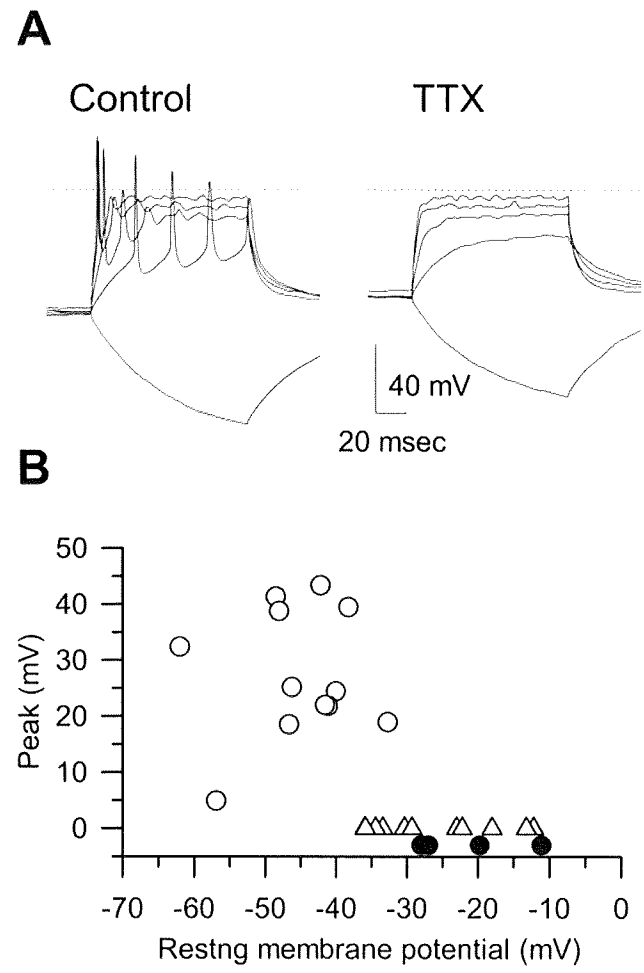

Figure 5. Electrophysiological properties of hES-derived neurons. (A): (Control) Action potentials elicited by depolarizing current injections (50 pA steps for 100 msec). The resting membrane potential was −62.0 mV. During the hyperpolarizing pulse (−50 pA), no 'sug' component was observed. (TTX) Membrane potentials recorded in the presence of 1 μM tetrodotoxin. In both panels, the dotted lines indicate 0 mV. (B): Summary of the resting membrane potentials and the peak amplitudes. Open circle; cells with action potentials. Open triangle; cells with action potentials only when the resting membrane potential was set to −70 mV. Closed circle; cells without membrane excitability.
doi:10.1371/journal.pone.0006318.g005

Discussion

We have shown in this study that neurons and astrocytes can be produced efficiently from hES cells using a conditioned medium collected from either rat primary-cultured astrocytes or hES cell-derived astrocytes. Astrocytes derived from hES cells can be used for continuous generation of neurons. Although a number of media including serum-free media supplemented with various cytokines and/or growth factors have been developed [10,11] to keep a long-term culture of neuronal cells, synthetic culture systems can usually maintain neural cells stable for only few weeks. Although a conditioned medium of primary-cultured astrocytes can be effective in culturing neurons for a longer period of time, the use of primary astrocytes may not be practical due to a number of limitations, including restricted availability of neural tissues as source of astrocytes, and extensive time and effort to obtain astrocytes from living tissues. Additionally, it is very difficult to maintain a stable culture of primary cells in a culture vessel, and subculture of these cells is limited within few passages.

The properties of primary-cultured astrocytes vary depending on the maturation stage of the living body and the region of the living tissue from which the astrocytes are derived. In addition, when astrocytes are obtained from a living body, contamination with cells other than the desired astrocytes is inevitable. Thus, it is difficult to prepare a stable astrocyte-conditioned medium having substantially uniform quality. With our method, on the other hand, ES-ACM can efficiently induce differentiation of hES cells into neural cells. Moreover, large amounts of ES-ACM can be produced stably and readily. ES-ACM, like P-ACM, can keep neuron cultures stable for more than eight weeks until mature neuronal phenotypes are apparent. In addition, completely xeno-free ES-ACM can be generated from immature hES cells by culture in chemically defined medium. With this completely xeno-free ES-ACM, xeno-free neurons and astrocytes can repeatedly be produced. In our transplantation experiment, donor cells did not express undifferentiated markers, such as Oct-3 and SSEA-4. In addition, only few Ki-67 positive cells found in the vicinity of the grafts were hrGFP-negative. These cells were unlikely to be derived from donor cells. It is important to exclude tumorigenicity of neuronal cells derived with this xeno-free method in future

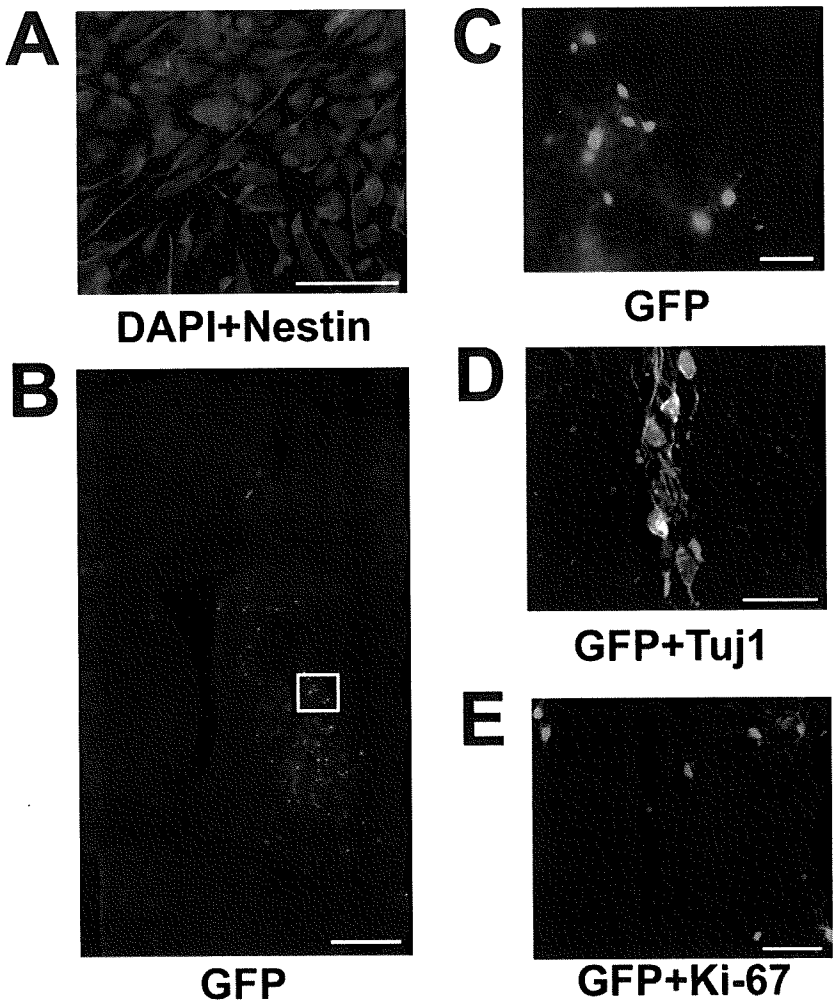

Figure 6. Survival of transplanted neural stem cells *in vivo*. (A): Most of the donor cells were confirmed to be Nestin-immunoreactve neural stem cells before transplantation. Anti-Nestin staining (green) and DAPI (blue). Bar = 50 μm. (B): Transplantation site. Grafted cells expressing hrGFP can be seen in the striatum. Bar = 500 μm. (C): High power magnification view of a white box in panel A. Some of the hrGFP-positive cells display a morphology similar to that of neurons. Bar = 50 μm. (D): Merged image of hrGFP expression (green) and immunostaining of anti-Tuj1 (red). Bar = 20 μm. (E): Merged image of hrGFP expression (green) and immunostaining of anti-Ki-67 (red). Bar = 50 μm.
doi:10.1371/journal.pone.0006318.g006

study for application to the cell therapy. Further studies are necessary to identify the specific molecules that induce neural cells in P- and ES-ACMs.

Recently, two methods adopting human tissue-derived cells have been reported as appropriate for clinical applications. One is an improved stromal cell-induced method that uses an amniotic membrane matrix [12]. The other uses telomerase-immortalized midbrain astrocytes [13]. Although both methods are xeno-free, they still need primary human tissues. On the other hand, with our method, neural cells can be induced from ES cells themselves. This self-serving method can supply donor cells consistently and may have an advantage for clinical applications.

Materials and Methods

ES cell culture

All experiments using hES cells were performed in conformity with "The Guidelines for Derivation and Utilization of Human Embryonic Stem Cells" of the Japanese government after approval by the institutional review board of Mitsubishi Tanabe Pharma Corporation. Two hES cell lines, SA002 and SA181, were obtained from Cellartis AB (Goteborg, Sweden) [14] and maintained on a mitotically inactivated mouse embryonic fibroblast feeder layer in a culture medium (vitroHES, Vitrolife AB, Goteborg, Sweden), supplemented with 4 ng/ml FGF-2 (Invitrogen, Carlsbad, CA). For passaging, the hES cells were treated with collagenase type IV (200 U/ml; Invitrogen) for 5 min, gently scraped from the culture dish, and then split 1:2–1:4 onto a feeder layer of mouse embryonic fibroblasts inactivated with 10 μg/ml mitomycin C.

Electroporation

All recombinant DNA experiments conformed to National Institute of Health (NIH) guidelines. First, a pGFP plasmid, in which hrGFP (Stratagene, La Jolla, CA) was expressed under the control of a CAG promoter (a gift from J. Miyazaki) [15] was constructed. Ten micrograms of the linearized plasmid was then electroporated into a suspension of hES cells (10^7 cells) in 0.8 mL of PBS using a Gene Pulser (500 μF, 250 V, Bio-Rad, Hercules, CA). The cells were next incubated on ice for 10 minutes, plated, and allowed to recover for 24 hours before selection with G418 (200 μg/mL). The cells were daily fed with the culture medium containing G418 for 12 days, after which the resulting ten G418-

resistant ES colonies showing strong hrGFP expression were individually picked and propagated. To analyze stem cell markers, alkaline phosphatase activity and cell surface markers were detected using an ES cell characterization kit (Chemicon, Temecula).

hES cell differentiation

Whole colonies of undifferentiated hES cells, 800–1000 μm in diameter, were picked up from the feeder layer using a glass capillary and transferred into non-adhesive bacteriological dishes each containing P-ACM supplemented with 20 ng/ml FGF-2 (R&D Systems Inc., Minneapolis). P-ACM was prepared as described previously [7]. The colonies were then cultured for 12 days, giving rise to spheres, which were next plated onto poly-L-Lysine/Laminin (Sigma-Aldrich, St. Louis) coated dishes and cultivated for seven days in NSCM (Neurobasal medium supplied with B27 supplement, both from Invitrogen, 20 ng/ml FGF-2, and 20 ng/ml recombinant EGF [R&D systems]). At this stage, the spheres gave rise to circular clusters of cells, many of which migrated from the clusters to the surrounding areas. After replacing the NSCM with P-ACM and culture for 14 days, the spheres differentiated into neurons and few astrocytes. To obtain more and purer neurons, the centers of the clusters containing undifferentiated ES cells were removed with a glass capillary, and the rest of the clusters were cultured for seven days in NSCM. Neuronal differentiation was then induced by subculture of neural stem cells using 0.05% Trypsin/EDTA in P-ACM for 14 days. To induce astrocytic differentiation, the neural stem cells were subcultured in G5 medium (Neurobasal medium supplemented with G5 supplement, both from Invitrogen, 10 ng/ml FGF-2, and 20 ng/ml EGF) for 14 days.

To induce astrocytic differentiation under xeno-free conditions, the colonies of hES cells were transferred into non-adhesive bacteriological dishes each containing N2 medium (Neurobasal medium supplied with N2 supplement, Invitrogen) supplemented with 20 ng/ml of FGF-2 and EGF. After the colonies were cultured for 12 days, few of them gave rise to spheres containing neural stem cells, which were subsequently plated onto poly-L-Lysine/Laminin in G5 medium. Centers of the spheres containing undifferentiated hES cells were removed with a glass capillary, and the rest of the clusters were cultured for seven days in G5 medium. By repeating over this cycle eight times, the spheres were purified to obtain pure neural stem cells. These neural stem cells were subcultured in G5 medium for 14 days to induce astrocytes. For collection of ES-ACM, hES cells derived-astrocytes were cultured in N2 medium for two days.

Immunostaining analysis

hES cells cultured in a 24-well plate were fixed in 4% paraformaldehyde in phosphate-buffered saline (PBS). Immunocytochemistry was performed using standard protocols and antibodies directed against Tuj1 (monoclonal 1:1000), MAP2 (monoclonal, 1:1000), GFAP (polyclonal 1:500), Oct-4 (monoclonal 1:500), SSEA-4 (monoclonal 1:400), Nestin (monoclonal 1:1000) (all from Chemicon), and TH (monoclonal, 1:400) (Acris Antibodies, Hiddenhausen, Germany). Alexa Fluor 594-labeled (Molecular Probes, Eugene, OR) and Cy3-labeled (GE healthcare, Uppsala, Sweden) secondary antibodies were used for visualization. 4′, 6-diamidino-2-phenylindole (DAPI, Kirkegaard Perry Laboratories, Gaithersburg) was used for nuclei staining.

Cell density of neural lineages (neurons and astrocytes) was determined by counting the numbers of DAPI, Tuj^+ and $GFAP^+$ cells per field at a magnification of 200 times using an inverted microscope. Five visual fields were randomly selected and counted for each sample. Numbers presented in figures represent the average percentage and SEM of positive cells over DAPI from three samples per each examination.

RT-PCR analysis

Total RNA was extracted from undifferentiated hES cells, neural stem cells, and neuronal cells using QIAshredder (QIAGEN, Hilden, Germany) and RNeasy Plus Mini kit (QIAGEN). Reverse transcription was carried out using random hexamers at 37°C for 60 minutes according to the manufacturer's instruction for First-Strand cDNA Synthesis Kit (GE Healthcare UK Ltd., Buckinghamshire, UK). PCR was carried out for 30 cycles using the specific primer sets. The reaction cycle was set at 95°C for 30 seconds, 55°C for 30 seconds, and 72°C for 30 seconds. The amplified fragments were subjected to electrophoresis in a 2% agarose gel, which was subsequently stained with ethidium bromide and photographed. The primers used are as follows: glyceraldelyde-3-phosphatedehydrogenase (GAPDH), ACCACAGTCCATGCCATCAC and TCCACCACCCTGTTGCTGTA; Oct4, CGTTCTCTTTGGAAAGGTGTTC and ACACTCGGACCACGTCTTTC; Nanog, AAGACAAGGTCCCGGTCAAG and CCTAGTGGTCTGCTGTATTAC; MAP2, CTTTCCGTTCATCTGCCATT and GCATATGCGCTGATTCTTCA; Nurr1, GCTAAACAAAACTTGCATGC and CTCATATCATGTGCCATACTAG; TH, GAGTACACCGCCGAGGAGATTG and GCGGATATACTGGGTGCACTGG; choline acetyltransferase (ChAT), ATGGGGCTGAGGACAGCGAAG and AAGTGTCGCATGCACTGCAGG; glutamic acid decarboxylase (GAD), ATTCTTGAAGCCAAACAG and TAGCTTTTCCCGTCGTTG.

Electrophysiology

The action potential was recorded using current clamp mode of Axopatch200B amplifier and Digidata 1320 interface (Axon, CA, USA). Physiological bathing solution contained (in mM); 140 NaCl, 5.4 KCl, 0.33 NaH_2PO_4, 0.5 $MgCl_2$, 1.8 $CaCl_2$, 5 HEPES (pH = 7.4 with NaOH). Standard high K^+ pipette solution contained; 110 Aspartic acid, 30 KCl, 5 MgATP, 5 Na_2 creatine phosphate, 0.1 Na_2GTP, 2 EGTA, 10 HEPES (pH = 7.2 with KOH). Electrode resistance was 8~6 MOhm. All experiments were carried out at 33–35°C.

Transplantation Experiment

Neural stem cells derived from hES cells using ES-ACM were implanted into the mouse striatum. All animal experimental protocols were approved by the Animal Ethics Committee of Mitsubishi Tanabe Pharma Corporation. 8-week-old C57BL/6 Cr Slc mice (SLC, Shizuoka, Japan) were anesthetized with pentobarbital and fixed on a stereotactic device (Narishige, Tokyo, Japan). By using a glass pipette with an inner diameter of 100 μm, 1×10^5 cells/5 μl were slowly (0.3 μl/min) injected into the striatum (AP±0 mm, ML +2.0 mm, DV −3.0 mm from bregma) of an adult male mouse. Four weeks after the transplantation, the recipient mouse was anesthetized with pentobarbital and perfused with ice-cold 4% paraformaldehyde in PBS. The brains of each mouse were postfixed in the same solution, cryoprotected with 30% sucrose in PBS for 48 h, and frozen. Coronal sections (thickness 40 μm) were cut on a microtome with freezing unit, collected in PBS (pH 7.4), and divided into series. Brain sections were incubated overnight with primary antibodies at 4°C. The primary antibodies used for immunohistochemistry ware mouse anti-Tuj1 (1:800, Covance, USA) and rabbit anti-Ki67 (1:25, abcam, UK). For detection of the primary antibodies, Alexa Fluor 594 goat anti-mouse IgG (1:1000; Molecular Probes) and Alexa

Fluor 594 goat anti-rabbit IgG (1:1000; Molecular Probes) were incubated with the samples. Immunoreactivity was assessed and viewed under confocal laser scanning microscopy (FV10i; Olympus, Tokyo).

Acknowledgements

We thank Jun-ichi Miyazaki, Osaka University Medical School, Osaka, Japan for the generous gift of plasmid pCAG. We also thank Naomi Takino and Hiroko Nishida, Division of Neurology, Department of Medicine, Jichi Medical University, Tochigi, Japan, for their technical assistance.

Author Contributions

Conceived and designed the experiments: TO HM SiM YK. Performed the experiments: TO NK HM KW MT. Analyzed the data: TO HM YS SN TI IN SiM MT YK. Contributed reagents/materials/analysis tools: TN SiM MT NI. Wrote the paper: TO SiM MT YK.

References

1. Thomson JA, Itskovitz-Eldor J, Shapiro SS, Waknitz MA, Swiergiel JJ, et al. (1998) Embryonic stem cell lines derived from human blastocysts. Science 282: 1145–1147.
2. Suemori H, Tada T, Torii R, Hosoi Y, Kobayashi K, et al. (2001) Establishment of embryonic stem cell lines from cynomolgus monkey blastocysts produced by IVF or ICSI. Dev Dyn 222: 273–279.
3. Bain G, Kitchens D, Yao M, Huettner JE, Gottlieb DI (1995) Embryonic stem cells express neuronal properties in vitro. Dev Biol 168: 342–357.
4. Okabe S, Forsberg-Nilsson K, Spiro AC, Segal M, McKay RD (1996) Development of neuronal precursor cells and functional postmitotic neurons from embryonic stem cells in vitro. Mech Dev 59: 89–102.
5. Kawasaki H, Mizuseki K, Nishikawa S, Kaneko S, Kuwana Y, et al. (2000) Induction of midbrain dopaminergic neurons from ES cells by stromal cell-derived inducing activity. Neuron 28: 31–40.
6. Tropepe V, Hitoshi S, Sirard C, Mak TW, Rossant J, et al. (2001) Direct neural fate specification from embryonic stem cells: a primitive mammalian neural stem cell stage acquired through a default mechanism. Neuron 30: 65–78.
7. Nakayama T, Momoki-Soga T, Inoue N (2003) Astrocyte-derived factors instruct differentiation of embryonic stem cells into neurons. Neurosci Res 46: 241–249.
8. Nakayama T, Momoki-Soga T, Yamaguchi K, Inoue N (2004) Efficient production of neural stem cells and neurons from embryonic stem cells. Neuroreport 15: 487–491.
9. Nakayama T, Sai T, Otsu M, Momoki-Soga T, Inoue N (2006) Astrocytogenesis of embryonic stem-cell-derived neural stem cells: Default differentiation. Neuroreport 17: 1519–1523.
10. Bottenstein JE, Sato GH (1979) Growth of a rat neuroblastoma cell line in serum-free supplemented medium. Proc Natl Acad Sci U S A 76: 514–517.
11. Brewer GJ, Cotman CW (1989) Survival and growth of hippocampal neurons in defined medium at low density: advantages of a sandwich culture technique or low oxygen. Brain Res 494: 65–74.
12. Ueno M, Matsumura M, Watanabe K, Nakamura T, Osakada F, et al. (2006) Neural conversion of ES cells by an inductive activity on human amniotic membrane matrix. Proc Natl Acad Sci U S A 103: 9554–9559.
13. Roy NS, Cleren C, Singh SK, Yang L, Beal MF, et al. (2006) Functional engraftment of human ES cell-derived dopaminergic neurons enriched by coculture with telomerase-immortalized midbrain astrocytes. Nat Med 12: 1259–1268.
14. Heins N, Englund MC, Sjoblom C, Dahl U, Tonning A, et al. (2004) Derivation, characterization, and differentiation of human embryonic stem cells. Stem Cells 22: 367–376.
15. Niwa H, Yamamura K, Miyazaki J (1991) Efficient selection for high-expression transfectants with a novel eukaryotic vector. Gene 108: 193–199.

Multitracer Assessment of Dopamine Function After Transplantation of Embryonic Stem Cell-Derived Neural Stem Cells in a Primate Model of Parkinson's Disease

SHIN-ICHI MURAMATSU,[1]* TSUYOSHI OKUNO,[2] YUTAKA SUZUKI,[2] TAKASHI NAKAYAMA,[3] TAKEHARU KAKIUCHI,[4] NAOMI TAKINO,[1] ASAKO IIDA,[1] FUMIKO ONO,[5] KEIJI TERAO,[5] NOBUO INOUE,[6] IMAHARU NAKANO,[1] YASUSHI KONDO,[2] AND HIDEO TSUKADA[4]

[1]*Divison of Neurology, Department of Medicine, Jichi Medical University, Tochigi 329-0498, Japan*
[2]*Mitsubishi Tanabe Pharma Corporation, Osaka 532-8505, Japan*
[3]*Department of Biochemistry I, Yokohama City University School of Medicine, Kanagawa 236-0004, Japan*
[4]*Central Research Laboratory, Hamamatsu Photonics K.K., Shizuoka 434-8601, Japan*
[5]*Tsukuba Primate Research Center, National Institute of Biomedical Innovation, Ibaraki 305-0843, Japan*
[6]*Division of Regenerative Neurosciences, Tokyo Metropolitan University, Tokyo 116-8551, Japan*

KEY WORDS ES cell; PET; monkey; MPTP

ABSTRACT The ability of primate embryonic stem (ES) cells to differentiate into dopamine (DA)-synthesizing neurons has raised hopes of creating novel cell therapies for Parkinson's disease (PD). As the primary purpose of cell transplantation in PD is restoration of dopaminergic neurotransmission in the striatum, in vivo assessment of DA function after grafting is necessary to achieve better therapeutic effects. A chronic model of PD was produced in two cynomolgus monkeys (M-1 and M-2) by systemic administration of neurotoxin. Neural stem cells (NSCs) derived from cynomolgus ES cells were implanted unilaterally in the putamen. To evaluate DA-specific functions, we used multiple [^{11}C]-labeled positron emission tomography (PET) tracers, including [β-^{11}C]L-3,4-dihydroxyphenylalanine (L-[β-^{11}C]DOPA, DA precursor ligand), [^{11}C]-2β-carbomethoxy-3β-(4-fluorophenyl)tropane ([^{11}C]β-CFT, DA transporter ligand) and [^{11}C]raclopride (D_2 receptor ligand). At 12 weeks after grafting NSCs, PET demonstrated significantly increased uptake of L-[β-^{11}C]DOPA (M-1:41%, M-2:61%) and [^{11}C]β-CFT (M-1:31%, M-2:36%) uptake in the grafted putamen. In addition, methamphetamine challenge in M-2 induced reduced [^{11}C]raclopride binding (16%) in the transplanted putamen, suggesting release of DA. These results show that transplantation of NSCs derived from cynomolgus monkey ES cells can restore DA function in the putamen of a primate model of PD. PET with multitracers is useful for functional studies in developing cell-based therapies against PD. **Synapse 63:541–548, 2009.**

INTRODUCTION

In Parkinson's disease (PD), the cardinal symptoms such as rest tremor, muscular rigidity and bradykinesia, become apparent after 40–50% of the neurons in the substantia nigra pars compacta (SNc) have been lost and striatal dopamine (DA) has been reduced to about 20% of normal levels (Kish et al., 1988). As a treatment for advanced PD, neural transplantation has been investigated for more than two decades with the aim of replacing degenerated DA neurons and restoring dopaminergic neurotransmission in the striatum. Embryonic stem (ES) cells may offer a substitute for currently used fetal midbrain cells, because they can proliferate extensively in an undifferentiated state and may provide an unlimited source of DA neurons (Li et al., 2008; Newman and Bakay, 2008). Transplantation of DA neurons derived from mouse ES cells

Contract grant sponsors: Ministry of Health, Labor and Welfare of Japan, Ministry of Education, Culture, Sports, Science and Technology of Japan (Special Coordination Funds), Japan Society for the Promotion of Science (Grant-in-Aid for Creative Scientific Research), CREST, the Japan Science and Technology Agency (JST).

*Correspondence to: Shin-Ichi Muramatsu, Division of Neurology, Department of Medicine, Jichi Medical University, 3311-1 Yakushiji, Shimotsuke, Tochigi 329-0498, Japan. E-mail: muramats@ms.jichi.ac.jp

Received 18 August 2008; Accepted 31 October 2008

DOI 10.1002/syn.20634

Published online in Wiley InterScience (www.interscience.wiley.com).